論文題目(Title of Thesis)　Recurrent CDC25C mutations drive malignant transformation in FPD/AML

（家族性血小板異常症の進展に際し頻発するCDC25C遺伝子変異による腫瘍化機構の解析）

氏　　名(Name)　　遠矢　嵩 Toya Takashi

追加情報(Additional information)：

この論文の一部は以下のように出版されています。
Nat Commun. 2014 Aug 27;5:4770. doi: 10.1038/ncomms5770.
Recurrent CDC25C mutations drive malignant transformation in FPD/AML.

In, the author's accepted manuscript is included.
The article was published in Nat Commun. 2014 Aug 27;5:4770.
The final version published is available online at
http://www.nature.com/ncomms/2014/140827/ncomms5770/full/ncomms5770.html.

博士論文

Recurrent CDC25C mutations drive malignant transformation in FPD/AML

（家族性血小板異常症の進展に際し頻発する CDC25C 遺伝子変異による腫瘍化機構の解析）

遠　矢　　嵩

Recurrent CDC25C mutations drive malignant transformation in FPD/AML

家族性血小板異常症の進展に際し頻発する CDC25C 遺伝子変異による腫瘍化機構の解析

東京大学大学院博士課程医学系研究科内科学専攻血液・腫瘍病態学

指導教員：黒川 峰夫

遠矢　嵩

Abstract

Familial platelet disorder with predisposition to acute myelogenous leukemia (FPD/AML) is an inherited disorder characterized by platelet defects and hematological malignancies whose molecular pathogenesis is poorly understood, except for germline mutations of *RUNX1*. We conducted a nationwide survey and 7 out of 57 pedigrees with familial thrombocytopenia or hematological disorder were diagnosed as FPD/AML. In these pedigrees, 7 out of 13 patients had developed hematological malignancies. The mutational spectrum of FPD/AML was obtained by whole-exome sequencing and deep sequencing, and we identified *CDC25C* as a recurrent target mutated in 7 of 13 (53 %) individuals, including 3 patients without malignancies. *GATA2* mutations were subclonal in 3 of 7 individuals with *CDC25C* abnormalities. Functional assays showed that mutated CDC25C disrupts the G2/M checkpoint, which accelerates genomic instability via RUNX1-mediated DNA damage. Prediction of hierarchical progression unveiled that *CDC25C* mutations form a founding pre-leukemic clone, followed by stepwise acquisition of mutations such as *GATA2* alterations. These findings suggest a role for impaired CDC25C functions in the transformation of FPD/AML.

Introduction

Familial platelet disorder with predisposition to acute myelogenous leukemia (FPD/AML) is an autosomal dominant disorder and is characterized by inherited mild to moderate thrombocytopenia with or without impaired platelet function and a lifelong risk of development into hematological malignancies such as myelodysplastic syndrome (MDS) and AML[1,2]. FPD/AML is so scarce that only about 30 pedigrees have been reported in the world and many clinical and etiological questions remain to be elucidated. A heterozygous germline mutation of *RUNX1* (*AML1*, *CBFA2*) gene on chromosome 21q22.3 is known to be the cause of this disease. RUNX1 is a transcription factor which is important for self-renewal of hematopoietic stem/progenitor cells and hematopoietic cell differentiation such as megakaryopoiesis. As Ichikawa and colleagues reported that loss of Runx1 in adult mice induced prominent thrombocytopenia[3], impaired platelet differentiation of patients with FPD/AML is considered to be caused by RUNX1 loss-of-function mutation. On the other hand, somatic *RUNX1* mutation is frequently observed in sporadic MDS and AML. RUNX1 mutations were revealed to evoke disrupted differentiation and increased self-renewal capacity of hematopoietic stem/progenitor cells and induce increase in immature hematopoietic cells in the bone marrow[3-5]. In addition, *RUNX1* mutation in AML is reported to be related to low remission rate and worse prognosis in some clinical trials[6-8]. Many of the RUNX1 mutations in sporadic MDS/AML as well as FPD/AML are located at the Runt-homology domain which is involved in DNA binding, although mutations in the transactivation domain or other region are also found in some cases[4].

Although inherited *RUNX1* mutation is the cause of thrombocytopenia, secondary mutations may have a role in the development and progression of hematological malignancies in

FPD/AML, as only about 40 % of FPD/AML patients develop leukemia with a median age of 33 years[9,10]. For example, given the differentiation block capacity of *RUNX1* mutation, additional mutation with proliferative potential may contribute to leukemogenesis in FPD/AML, as some growth-stimulative gene alteration is expected to be necessary as a partner genetic change with *RUNX1* mutation in sporadic MDS/AML[11,12]. Molecular pathogenesis of this disorder has not been fully elucidated and the lack of the pathognomonic mutations has impeded the clinical improvement to refine cancer diagnosis and to identify patients at risk for onset of malignancies in FPD/AML. To address these issues, we conducted a nationwide survey in Japan to collect samples and make a diagnosis of patients with familial thrombocytopenia or hematological malignancies and applied a high-throughput sequencing strategy to hematological malignancies in FPD/AML, with the aim of identifying novel recurrent driver mutations.

Materials and Methods

Subjects

Studies involving human subjects were done in accordance with The Ethics Guidelines for Human Genome/Gene Analysis Research, which was developed by the Ministry of Health, Labour and Welfare, Japan, the Ministry of Education, Culture, Sports, Science, and Technology, Japan, and the Ministry of Economy, Trade, and Industry, Japan, and enforced on March 29, 2001. This study was approved by ethical committee of the University of Tokyo (approval number; 3211) and each participating institutions. Written informed consent was obtained from all patients whose samples were collected after the guideline was enforced. All animal experiments were approved by the University of Tokyo Ethics Committee for Animal Experiments. The clinical data, peripheral blood sample and buccal mucosa of the patients were collected from participating institutions. When a *RUNX1* mutation was detected in genomic DNA from buccal mucosa and peripheral blood, the patient was considered as having FPD/AML.

Nationwide survey

We first sent questionnaires to 489 institutions in Japan to investigate pedigrees with familial thrombocytopenia or hematological malignancy. Familial MDS or leukemia pedigrees were also included in this nationwide survey because FPD patients were sometimes diagnosed only after MDS or leukemia progression. Of these institutions, 400 (81.8%) responded and 80 pedigrees were yielded. We sent second questionnaires to the institutions to request the information about the clinical features, complications, family history, complete blood count, results of bone marrow examination, treatment and clinical outcome. In addition to clinical

data, peripheral blood and buccal mucosa samples were also offered when written informed consent for sample collection and mutation analyses were obtained.

For acquired samples, genomic DNA was extracted using a QIAamp DNA Mini kit (Qiagen). Direct sequencing for *RUNX1* and other genes related to MDS or familial thrombocytopenia (*MPL*, *MYH9*, *MYL9*, *GATA1*, *GATA2*, *GP1BA*, *GP9*, *MASTL*, *HOXA11*, *CEBPA*, *CBL*, *DIDO1*, *ANKRD26*) were underwent and mutation status were analyzed.

Whole exome sequencing

Genomic DNA was extracted from the bone marrow samples of the two patients in MDS/MF and AML phase (Subject 20 and Subject 21) using the QIAamp DNA Mini kit (Qiagen). Exome capture was performed and Enriched exome fragments were subjected to sequencing using the Solexa platform (Illumina). All candidate mutations which were predicted to be deleterious by the Polyphen-2 algorithm were validated by Sanger sequencing. Genomic DNA samples from the buccal mucosa of the two patients (Subject 20 and Subject 21) were also extracted using a QIAamp DNA Mini kit (Qiagen). They were considered as references, and the mutations were judged as somatic mutations when they were not detected in buccal mucosa genomic DNA by Sanger sequencing. All candidate somatic mutations were also validated by Sanger sequencing and deep resequencing using primers listed in **Table 1 and Table 2**.

Table 1. List of PCR primers used for validation by Sanger sequencing.

Target	Forward primer (5'→3')	Reverse primer (5'→3')
AGAP4	TGCGAGAGCAGTAAAAGCAA	TGCTGTTGGCTAGGTCATTG
ANXA8L1	GGTGAGGCAGGATTGTTGAT	GTCTCTGCATCTCCCCTCTG
CDC25C	TGCAGACACACTTGGAGGAG	CCTTCCTGAGCTTTCCTTGG
CHEK2	TGTCTTCTTGGACTGGCAGA	CAGGAGGCAGAGGCTACAGT
COL9A1	AGTCATCATCCATCGCTTCC	TCAGGCCCTTTGTTAAATGC
DENND5A	CACCCTCAAGGGAATCACAT	CCCATCAGGTATGGAACAGG
DTX2	TCTGCAGGGCTACTGATGTG	GACAAACTGCTGCTCGATGA
FAM22G	CAGAGCCACACCCTCTCTCT	AAAAGCACAGCAGGGTCTTC
FER	GGTCCTGGAACCAGTCTCCT	CGAGGAGAAATCAAAGAGATCG
FNDC1	TGTGGGGAGGAATATGTGGT	AGGAGAAAACCCCGTGATCT
GATA2	AGACCCTCTCGTCCCTCTTC	AGACGACCCCAACTGACATC
LPP	TCACCTCGCCAAATATCACA	TGGAAATCTCGATCCAAAGC
OR8U1	TCCTTGCTACTGGCTTCCAT	CTCAGCTGAATGCATCCTCA
PIDD	TCCGACACCTTCTCCAGAGT	CAAGGATGGTGTGAGCACTG
RP1L1	AGGCTGCTACCTCTGCTCTG	AGACCCCAACAGCCTACCTT
SIGLEC9	CCCATCCTCACTGTCTGCTC	TCCCTCAATCAGGGTGAGTC
ZNF614	GCAAGAGCACTCTCCAAACC	GGAAGGTTTGCTCACATTCAA

Table 2. List of PCR primers used for deep sequencing.

Target	Forward primer (5'→3')	Reverse primer (5'→3')
AGAP4	CCTAAGTGGGCCAGTTTGAA	TGCTGTTGGCTAGGTCATTG
ANXA8L1	CACACAGATCCGTCCATCAC	CTGAGGGTCTTGCCGTACAT
CHEK2	TATGTGGAACCCCCACCTAC	CCTACCAGTCTGTGCAGCAA
COL9A1	CCAGTTTGCATCAATGAGGA	AGGCTGGCTCACAGAAACC
DENND5A	CACCCTCAAGGGAATCACAT	CTCCGCCACAGTCATCAGT
DTX2	CTGAAGCTGTTTGGGAAAGC	GACAAACTGCTGCTCGATGA
FAM22G	GTAAGTGCCCCCTTTCCTTC	ACCTCTCTCGCTGCTTCTTG
FER	GAGTTTGCACACAAAGACAGC	CCTTGGAGACTTTACGAGGAGA
FNDC1	CTGTCTGGAGCCAAGAGTCC	GATCCCAAAGACCATGGAAA
GATA2	GAGAACTTGCCGGTTAAGCA	TGCCCATTCATCTTGTGGTA
LPP	GTGTCGACGCGCAGTATCTA	TGGAAATCTCGATCCAAAGC
OR8U1	TCACACCATCCTCACCTTCC	TGATACCAGCACAGGCAAAG
PIDD	GTCCAGGCTCCAACACGTAG	CCGATAGCGGATGGTGAT
RP1L1	AGGAGAGAAACCCCACTGCT	GCGGCCAGGTTCCTAGTATT
SIGLEC9	GGGGAAGGAGAGCTCCAGTA	TCCCTCAATCAGGGTGAGTC
ZNF614	TTCCAAGTCTTCAAGCATCAGA	CACATTGACCACTTCCAGGAT
CDC25C_ex1	CTCCTGGTGAGAATTCGAAGA	CCCAACTGTTTGGAAATAGCA
CDC25C_ex2	AATCTAATGGGAATTTCGATGTACT	TTCTTCCCTTTGAGGCCTTT
CDC25C_ex3	AGGAAAAACAGGATGCATGG	GCTTTTGTGTGGGGTTCATT
CDC25C_ex4	AAATGTTGGGATGCACCAAT	AGGTGCAATGGAAACCCTCT
CDC25C_ex5	TTGAGGATGCTGGACGTTCT	CTGCCAATATATCTAGGTTTCCA
CDC25C_ex6	TGGTGGCATTATCCAAATCC	CCACAGAACACTTTACCTTTGC
CDC25C_ex7	TGAGCAGAAGTGGCCTATATC	CTTCCTGAGCTTTCCTTGG
CDC25C_ex8	CCACTCCATCCACTGGTTTT	ACAGGATGGGTGTAGCCAAA
CDC25C_ex9	TGGGTGTGGAATACTTGCTG	TGGGCATTTTAGGGACAGAA
CDC25C_ex10	TGACCCTTCTCTCCCTCAGA	CTCCCCTACTAATGGCCACA
CDC25C_ex11	AAGCCCCTGAGGAAATACTTA	GCCAGACCCCATTTAGACAC
CDC25C_ex12	CACCCATCTCTGGGTTCTCT	GCCCTGGGAGTTGAGTTGT
CDC25C_ex13	TCCCTTACTCTGTTCCTTACCTTT	GCCAGTGGCTGGAATGTTA

Deep sequencing

Genomic DNA was extracted from bone marrow samples of two FPD patients (Subject 20 and Subject 21) at AML phase and peripheral blood samples of patients who was diagnosed as FPD but had not developed hematological malignancies. Each targeted region was PCR amplified with specific primers (**Table 2**) and the amplification products from an individual sample were combined and purified with AMpure XP Kit (Beckman Coulter) and library preparation was carried out using the Ion Xpress™ Fragment Library Kit (Life Technologies) according to the manufacturer's instructions. The Agilent 2100 Bioanalyzer (Agilent Technologies) and the associated High Sensitivity DNA kit (Agilent Technologies) were used to determine quality and concentration of the libraries. The amount of library required for template preparation was calculated using the Template Dilution Factor calculation described in the protocol. Emulsion PCR and enrichment steps were carried out using the Ion OneTouch 200 Template Kit v2 DL (Life Technologies). Sequencing was undertaken using Ion Torrent PGM and Ion 318 chips Kit v2 (Life Technologies). The Ion PGM 200 Sequencing Kit (Life Technologies) was used for sequencing reactions, following the recommended protocol. The presence of *CDC25C* and *GATA2* mutations was validated by a subclone strategy for DNA sequence analysis.

Subclone strategy and direct sequencing

Using genomic DNA of the patients as template, each targeted region was amplified by PCR with specific primers (**Table 2**). PCR products were purified with illustra ExoStar (GE Healthcare) and subcloned into EcoRV site of pBluescript II KS(-) (Stratagene). Ligated plasmids were transformed into *E. coli* strain XL1-Blue by 45 second heat shock at 42℃.

Transformed cells were incubated on LB plates containing 100 μg/ml ampicillin supplemented with X-gal (Sigma-Aldrich) and IPTG (Sigma-Aldrich). For colony PCR, a portion of a white colony was directly added to a PCR mixture as the DNA template. Insert region was amplified by PCR procedure with T3 and T7 universal primers, purified with illustra ExoStar, and sequenced by Sanger method with T3 and T7 primers using BigDye Terminator v3.1 Cycle Sequencing kit (Applied Biosystems) and ABI Prism 310 Genetic Analyzer (Life Technologies).

Single cell sequencing and genome amplification

Single cells were separated from the bone marrow of Subject 20 at AML phase using FACSAria II (BD biosciences). Each cell was deposited into individual wells of 96-well plate. Single cells were lysed and whole genome from single cell was amplified using GenomePlex Single Cell Whole Genome Amplification Kit (Sigma-Aldrich). Mutation status of genes were analyzed by direct sequencing with specific primers (**Table 3**). In order to improve the sensitivity of this procedure, we used multiple primer sets for detecting a single nucleotide variation. We estimated the false negative rate of this procedure based on the ratio of *RUNX1* mutation, which is supposed to be observed in all of the cells. The false negative rate was estimated to be 35 % (22 cells out of 63 cells), which is consistent with the manufacturer's bulletin reporting the allelic dropout of 30 %. In light of these results, we regard those cells with at least one gene mutation in a mutational group (colored in red, orange, green, blue, or purple) as being positive for gene mutations of the corresponding group.

Table 3. List of PCR primers used for single cell sequencing.

Target	Forward primer (5'→3')	Reverse primer (5'→3')
AGAP4	AAAACATGCGTGGGAACG	TGCTGTTGGCTAGGTCATTG
CDC25C_1	GGTTTAATATTCCCAAACAGGTG	GCAAAGACATGAGATAGAAGATGAA
CDC25C_2	TGCAGACACACTTGGAGGAG	CCTTCCTGAGCTTTCCTTGG
CDC25C_3	GAACAGGCCAAGACTGAAGC	CCAGAAAAGCAAAGACATGAGA
CHEK2_1	TTTTGGGCACTCCAAGATTT	CATTTGTGACTTCATCTAATCACCT
CHEK2_2	TGGCAAGTTCAACATTATTCC	CCTAAACTCCAGCAGTCCACA
CHEK2_3	CTGTTGGGACTGCTGGGTAT	CAGGAGGCAGAGGCTACAGT
COL9A1_1	CCAGTTTGCATCAATGAGGA	TCAGGCCCTTTGTTAAATGC
COL9A1_2	ATGCCCTCTGCCAGTTTG	AGGCTGGCTCACAGAAACC
COL9A1_3	CTGCCAGCTATGGCAGAAAT	TCAGGCCCTTTGTTAAATGC
DTX2	TGCTCATGTCTGTCCTGTTCA	CACTGTAGGGGTGCCAGGT
FAM22G_1	GGGCAGCGCCAGTAAGTG	CTGTCCCTGAGGGTCCTG
FAM22G_2	CCCTGGTCTCCACCATTCT	CAGCTGCAAACTCAGAAGGA
FAM22G_3	AAGCGCCTCCTGTCCTTG	ACTCTGCCCTGTCCCTGAG
GATA2_1	CCCTGTTCCCCTGCAGAA	AATTAACCGCCAGCTCCTG
GATA2_2	CCGTGTCTCTCCCTGTTCC	TAATTAACCGCCAGCTCCTG
GATA2_3	GAGAACTTGCCGGTTAAGCA	TGCCCATTCATCTTGTGGTA
GATA2_4	CTACCTGTGCAATGCCTGTG	AAAGCGTCTGCATTTGAAGG
LPP_1	TCCACCTCTTCCTTTTACCTC	TCGCATCGGTAGCAGTGA
LPP_2	TTACGGATGAGGAAGCAGGT	TGGCATAATAGGCTCCTTGC
LPP_3	GTGTCGACGCGCAGTATCTA	GCAGGGCTGTCAACCAGA
RP1L1_1	GGCTGCTACCTCTGCTCTGA	TGTGACTGAGAACCACTGTCTG
RP1L1_2	GATGGAGGCTGCTACCTCTG	GCGAGGGTCCATGTTCTTAAT
RP1L1_3	AGGAGAGAAACCCCACTGCT	GCGGCCAGGTTCCTAGTATT
RUNX1	TGGCTTCCCATCCTCCTA	GCGGCAGGTAGGTGTGGTA
SIGLEC9	GGCCCCTGACTGAACCTT	TCAGGGTGAGTCTCTGCAGTT

Immunoprecipitation and Western blotting

The experiments were performed as described previously[13]. Briefly, HEK293T cells were transiently transfected with mammalian expression plasmids encoding proteins of Flag-tagged CDC25C and its mutants, HA-tagged 14-3-3 or c-TAK1. All plasmids were sequence verified. 48 hours later, cell lysates were collected and incubated with anti-HA monoclonal antibody (MBL) for 1 hour. After incubation, the cell lysates were incubated with protein G-Sepharose (GE Healthcare) for 1 hour. The precipitates were washed twice with TNE buffer, twice with high salt-containing wash buffer, and once with low salt-containing buffer and analyzed by Western blotting. In immunoblotting, anti-Flag (Sigma-Aldrich), anti-HA (Roche), anti-CDC25C (Cell Signaling Technology), anti-phospho-CDC25C (Ser216) (Cell Signaling Technology) or anti-beta-actin (Cell Signaling Technology) antibodies were used. Immunostar LD (Wako) was used for detection and each protein level was normalized according to beta-actin expression level.

Retrovirus production

The procedures were performed as described previously[13]. Briefly, Plat-E packaging cells were transiently transfected with each retroviral constructs using calcium phosphate precipitation method, and supernatant containing retrovirus was collected 48 hours after transfection and used for infection after centrifuged for overnight at 10,000 rpm.

Cell cycle synchronization and analysis for mitosis entry

After transduction of wild-type CDC25C or its mutated forms, Ba/F3 cells were treated with 2 mM thymidine (Sigma-Aldrich) for 12 hours to obtain cell cycle synchronization at G1/S

phase. Then thymidine was washed out and the cells were incubated with 1 mM nocodazole (Sigma-Aldrich) with or without 2 Gy of irradiation. Cell cycle was analyzed over time as previously described[13]. To assess the cooperation of *CDC25C* and *RUNX1* mutation, wild-type or mutant (D234G, H437N) pMXs-neo-Flag-CDC25C and mutant (F303fsX566, R174X) pGCDNsam-IRES-KusabiraOrange-Flag-RUNX1 were retrovirally transduced into Ba/F3 cells.

Immunofluorescent microscopic analysis

Ba/F3 cells were fixed in 3.7% formaldehyde in PBS for 20 minutes. After washing with PBS, the cells were permeabilized with 0.2% Triton in PBS for 10 minutes, followed by blocking by treatment with 1% BSA in PBS for 40minutes. Staining for phosphorylated histone H2AX was performed with anti-phospho-histone H2AX (Ser139) antibody (dilution, 1:500; Merck Millipore) at room temperature for 3 hours. After washing with PBS three times and with 1% BSA in PBS, the cells were treated with Alexa Fluor 488 rabbit anti-mouse IgG (dilution, 1:500; Invitrogen) and TO-PRO3 (dilution, 1:1000; Molecular Probes) for 1 hour. The proteins were visualized using FV10i (Olympus). The percentage of γH2AX foci positive cells was determined by examining 100 cells per sample. Three independent experiments were performed. To evaluate the localization of CDC25C, Ba/F3 cells were treated with 2 mM thymidine for 12 hours and stained. The mean intensity of CDC25C in nucleus and cytoplasm of each cell was measured within a region of interest (ROI) placed within nucleus and cytoplasm. Similarly, the background intensity was quantified within ROI placed outside the cells. All the measurements were performed using the Fluoview FV10i software. The background-subtracted intensity ratio of nucleus to cytoplasm was calculated in more than 50

cells in each specimen.

Quantitative real-time PCR

RNA was extracted from each cells using NucleoSpin RNA II kit (Clontech) and complementary DNA was synthesized by ReverTra Ace qPCR RT Master Mix (TOYOBO). Real-time PCR was carried out using THUNDERBIRD SYBR qPCR mix (TOYOBO) and the LightCycler 480 Instrument II (Roche) according to the manufacturer's instructions. The results were normalized to 18s ribosomal RNA level.

Statistical analysis

To compare data between groups, unpaired Student t test was used when equal variance were met by F-test. When unequal variances were detected, the Welch t test was used. Differences were considered statistically significant at a p value of less than 0.05.

Results

Nationwide survey

As a result of our survey, answers for 56 patients from 50 pedigrees (57.5% of 80) and 54 samples from 45 pedigrees (56.2% of 80) were obtained, and seven pedigrees (Pedigree 16, 18, 19, 32, 53, 54 and 57) with germline *RUNX1* mutation were diagnosed as having FPD/AML, in which 7 out of 13 patients had developed hematological malignancies (**Table 4**). Although RUNX1_p.Met439I mutation was detected in an aplastic anemia patient (Subject 58), this mutation was shown as somatic mutation because the mutation was not detected in buccal mucosa. About 38 pedigrees without germline *RUNX1* mutation, mutation analyses targeting various genes related to familial thrombocytopenia, MDS or AML were underwent. As a result, 2 *MYH9* mutations in 2 pedigrees (p.Phe41Leu in pedigree 11 and p.Asp1424Asn in pedigree 21) and 1 *ANKRD26* mutation in 1 pedigree (c.-134G>A in pedigree 3) were detected. No responsible germline mutation was detected in other 35 pedigrees. Clinical data of 56 patients from 50 pedigrees were available. Median age at initial diagnosis was 38 years old (range; 0-80 years old. **Fig.1a**). 22 patients (39.2%) were male and 34 patients were female, and median platelet count was 5.9×10^{10}/L ($0.1\text{-}18.7\times10^{10}$/L, **Fig.1c**). Bleeding symptoms were observed for 13 patients (23.2%). We could not evaluate the platelet aggregation because it was not assessed in most patients. 25 patients (44.6%) were diagnosed as having immunothromboctopenic purpura (ITP) at initial medical examination and 16 patients (28.5%) were diagnosed hematological malignancy (8 with MDS, 3 with AML and 5 with lymphoid malignancy, **Fig.1b**). 9 patients (16.0%) were diagnosed or suspected to be FPD/AML at initial diagnosis. However, only 2 patients out of the 9 patients actually had *RUNX1* germline mutation. Other 7 patients were considered as ITP (2 patients), AA (2 patients), MDS (1 patient), AML (1 patient) or hairy cell leukemia (1 patient). Among 25 patients who were diagnosed as ITP at initial examination, three patients suffered from MDS later. In this survey, no patient was

transfusion-dependent with the exception of patients with hematological malignancy.

For 42 patients with both clinical data and samples available, platelet count at initial examination was not significantly different between patients with germline *RUNX1* mutation and patients without the mutation (p=0.46, **Fig.1d**). Gender, bleeding symptom and age at diagnosis were also comparable (p=0.62, 0.95 and 0.39, **Fig.1e**).

Table 4. Mutational status of *CDC25C* in FPD/AML patients

Pedigree number	Subject number	RUNX1 mutation	Disease status	Age[a]	CDC25C mutation	VAF (%)
18	20	p.Phe303fs	MDS	37	p.Asp234Gly	31.7
			AML	38	p.Asp234Gly	45.8
	21		MF	17	p.Asp234Gly	31.1
			AML	18	p.Asp234Gly	39.0
19	22	p.Arg174*	AML	41	p.His437Asn	39.7
54	65	p.Ser140Asn	MDS	25	-	-
	66		AML	56	p.Asp234Gly	24.2
32	38	p.Leu445Pro	HCL	72	-	-
16	18	p.Thr233fs	Thrombocytopenia	-	p.Asp234Gly	5.9
53	62	p.Gly262fs	MDS	12	-	-
	63		Thrombocytopenia	-	-	-
	67		Thrombocytopenia	-	-	-
57	71	p.Gly172Glu	Pancytopenia[b]	-	p.Asp234Gly	8.3
	72		Thrombocytopenia	-	-	-
	73		Thrombocytopenia	-	p.Lys233Glu	1.8

HCL, hairy cell leukemia, VAF, variant allele frequency

[a]Age at the time of diagnosis of haematological malignancy is shown.

[b]Thrombocytopenia, leukopenia, and iron-deficiency anemia were diagnosed.

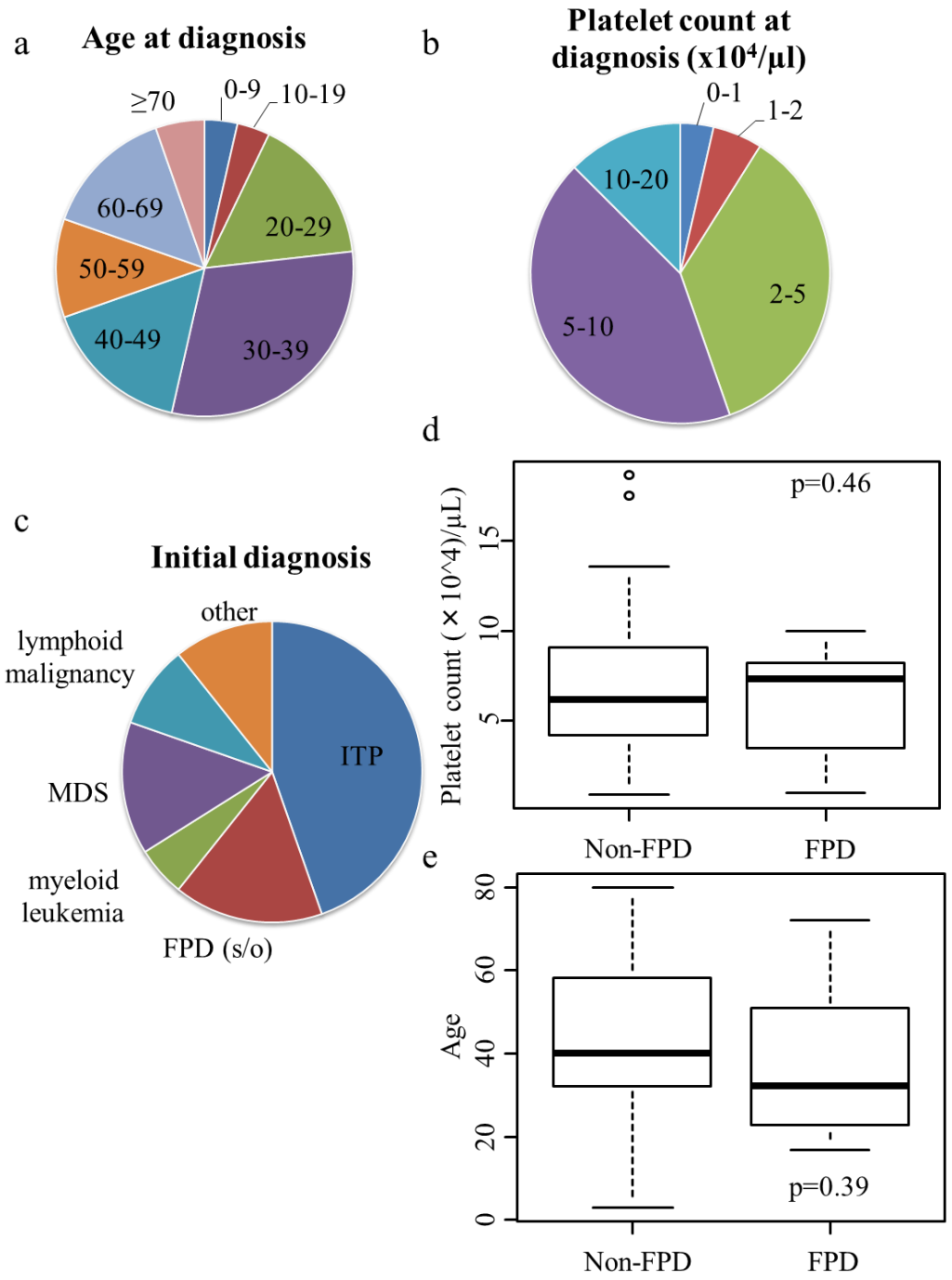

Figure 1.
Results of nationwide survey: clinical characteristics of patients with familial thrombocytopenia or hematological malignancies. (**a**) Age at diagnosis of patients (n=56). (**b**) Platelet count at initial diagnosis (n=56). (**c**) Initial diagnosis of patients (n=56). (**d**) Comparison of platelet count at initial diagnosis between patients with germline *RUNX1* mutation and without mutation (n=42). (**e**) Comparison of age at initial diagnosis between patients with germline *RUNX1* mutation and without mutation (n=42).

Recurrent *CDC25C* mutation in FPD/AML patients

To systematically identify additional genetic alterations, we utilized whole-exome sequencing in 2 patients with FPD/AML who had RUNX1_p.Phe303fs mutation and developed myelodysplastic syndrome (MDS) (Subject 20) or myelofibrosis (MF) (Subject 21) followed by AML development[14]. Validation by Sanger sequencing and/or deep resequencing of candidate genes in tumor and normal DNA confirmed 10 and 8 somatically acquired nonsynonymous mutations in these patients, respectively (**Table 5, Fig. 2, 3 and 4**). It is intriguing to note that these patients had a common somatic *CDC25C* mutation affecting p.Asp234, which had not been reported in hematological malignancy (**Fig. 5**). As recurrently affected genes are of primary interest in identifying driver mutations, the other individuals with FPD/AML were vigorously investigated by deep sequencing to determine the frequency of mutations in *CDC25C* in patients with the disease and further validated by a subclone strategy for DNA sequence analysis. As a result, 4 further *CDC25C* somatic mutations were identified in the 8 affected individuals with hematological malignancy and, interestingly, 3 mutations were detected in 5 individuals *without* malignancy (**Fig. 6a and Table 4**). Thus, 7 out of 13 affected individuals harbored *CDC25C* mutations, for an overall occurrence rate of 54 %.

Table 5. Validated somatic mutations.

GeneSymbol	RefSeq_no.	Amino acid change	Position (hg19)	Base change	Mutation type	Polyphen2 prediction	SIFT prediction	VAF at MDS/MF	VAF at AML
Subject 20									
AGAP4	NM_133446	p.Arg484Cys	g.chr10:46321905	C->T	Missense	Damaging	Damaging	13.2 %	11.5 %
CDC25C	NM_001790	p.Asp234Gly	g.chr5:137627720	A->G	Missense	Damaging	Damaging	31.7 %	45.8 %
CHEK2	NM_007194	p.Arg406His	g.chr22:29091740	G->A	Missense	Damaging	Tolerated	14.6%	11.1 %
COL9A1	NM_001851	p.Gly878Val	g.chr6:70926733	G->T	Missense	Damaging	Damaging	9.6 %	26.4 %
DTX2	NM_001102594	p.Pro74Arg	g.chr7:76110047	C->G	Missense	Damaging	Damaging	18.3 %	11.2 %
FAM22G	NM_001170741	p.Ser508Thr	g.chr9:99700727	T->A	Missense	Damaging	Tolerated	10.2 %	27.6 %
GATA2	NM_001145661	p.Leu321His	g.chr3:128202758	T->A	Missense	Damaging	Damaging	0.0 %	28.1 %
LPP	NM_001167671	p.Val538Met	g.chr3:188590453	G->A	Missense	Damaging	Damaging	9.7 %	28.8 %
RP1L1	NM_178857	p.Ser215fs	g.chr8:10480295	insC	frameshift	Damaging	Damaging	14.2 %	12.7 %
SIGLEC9	NM_014441	p.Ser437Gly	g.chr19:51633253	A->G	Missense	Damaging	Tolerated	27.4 %	42.5 %
Subject 21									
ANXA8L1	NM_001098845	p.Val281Ala	g.chr10:48268018	T->C	Missense	Damaging	Damaging	30.8 %	36.8 %
CDC25C	NM_001790	p.Asp234Gly	g.chr5:137627720	A->G	Missense	Damaging	Damaging	31.1 %	39.1 %
DENND5A	NM_001243254	p.Arg320Ser	g.chr11:9215218	A->C	Missense	Damaging	Damaging	29.5 %	37.3 %
FER	NM_005246	p.Tyr634Cys	g.chr5:108382876	A->G	Missense	Damaging	Damaging	1.4 %	30.4 %
FNDC1	NM_032532	p.Arg189Cys	g.chr6:159636081	C->T	Missense	Damaging	Damaging	29.3 %	35.9 %
OR8U1	NM_001005204	p.Asn175Ile	g.chr11:56143623	A->T	Missense	Damaging	Damaging	30.0 %	34.1 %
PIDD	NM_145886	p.Arg342Cys	g.chr11:802347	C->T	Missense	Damaging	Damaging	3.3 %	28.3 %
ZNF614	NM_025040	p.Glu202Gly	g.chr19:52520246	A->G	Missense	Damaging	Damaging	28.7 %	33.7 %

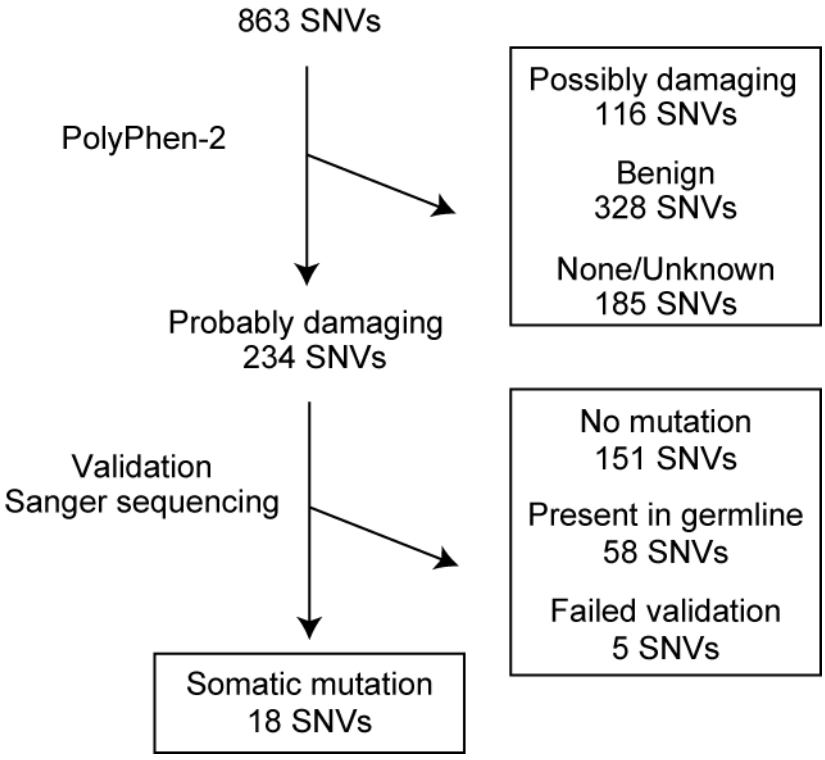

Figure 2.
Prioritization scheme for validation of SNVs. Filter scheme for discovery of SNVs. 234 SNVs were sent for validation from germline, pre-leukemic phase, and leukemic phase sample genomic DNA. 18 SNVs were validated (not present in germline), 151 SNVs did not validate (wild type sequence instead at predicted site), and 5 SNVs failed during the validation process and no data was available after Sanger sequencing.

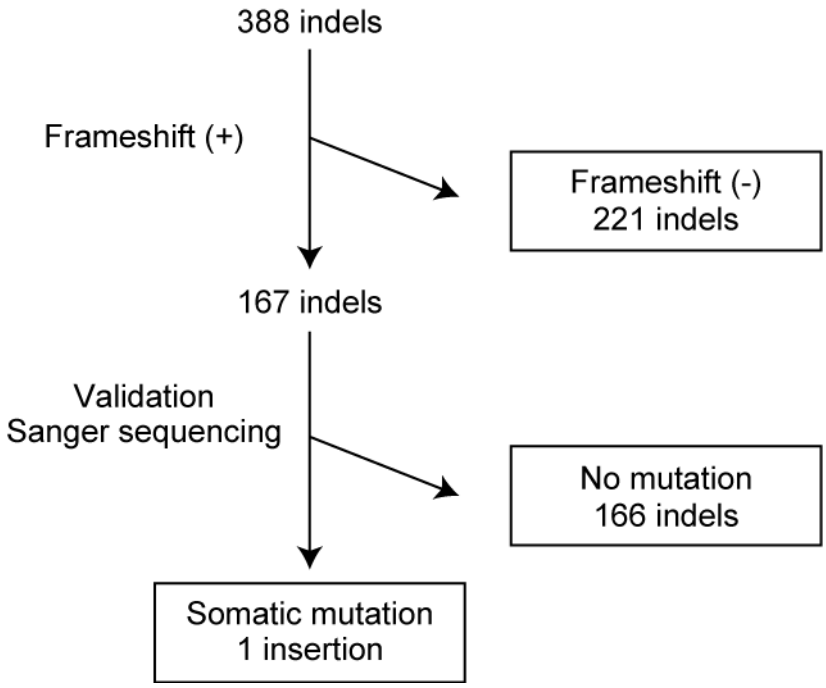

Figure 3.
Prioritization scheme for validation of indels. Filter scheme for discovery of indels. 167 candidate indels with frameshift were sent for validation from germline, pre-leukemic phase, and leukemic phase sample genomic DNA. 1 insertions were validated (not present in germline) and 166 SNVs did not validate (wild type sequence instead at predicted site).

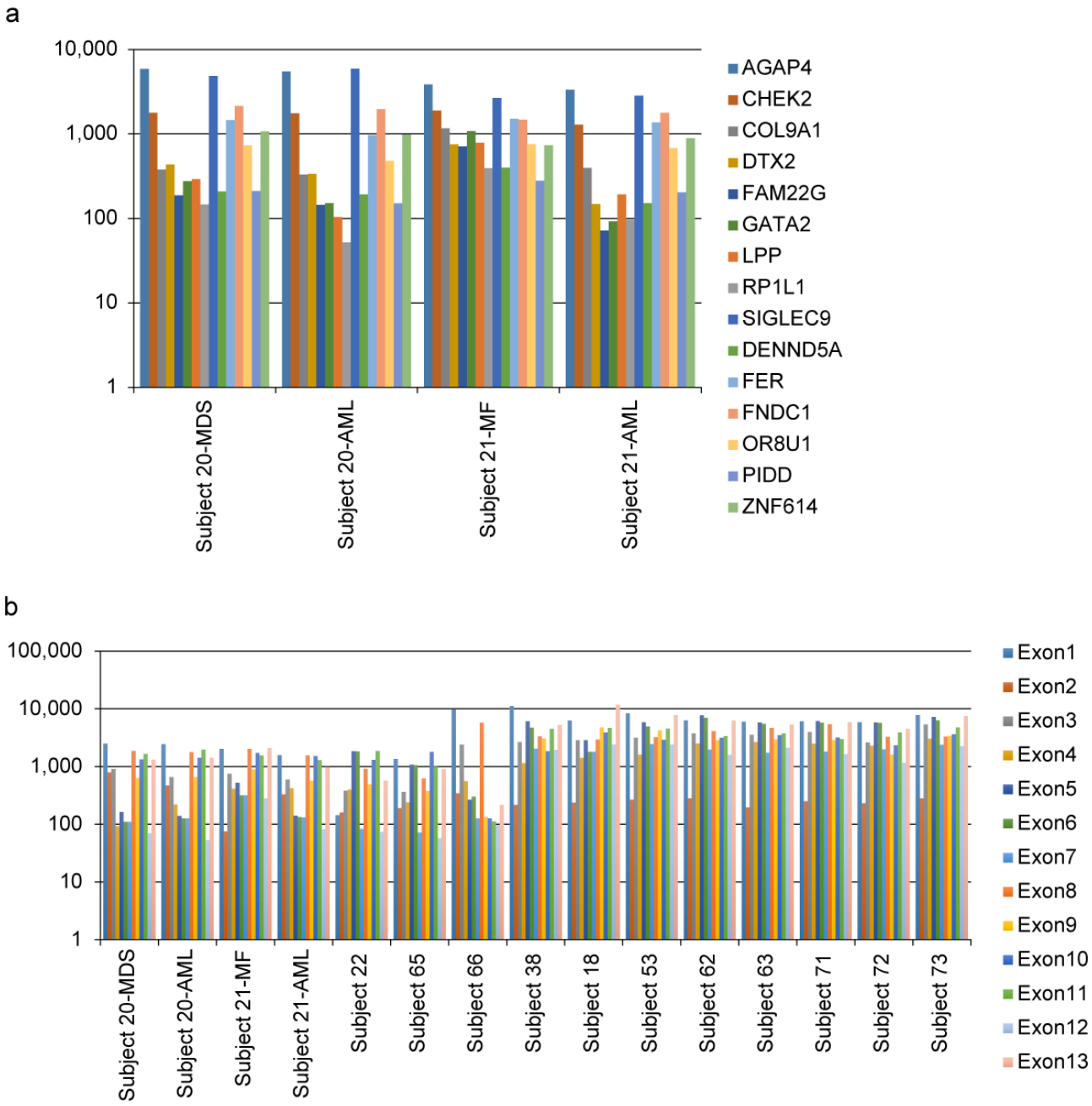

Figure 4.

Mean coverage of targeted deep sequencing. (**a**) Mean coverage of deep resequencing of targeted genes (except *CDC25C*) in Subject 20 and 21 at pre-leukemic phase or leukemic phase is shown, respectively. (**b**) Mean coverage of deep resequencing of *CDC25C* in each sample is shown. The mean value of exon 1-13 in each sample was displayed (the result of 15 specimens from 13 patients in total).

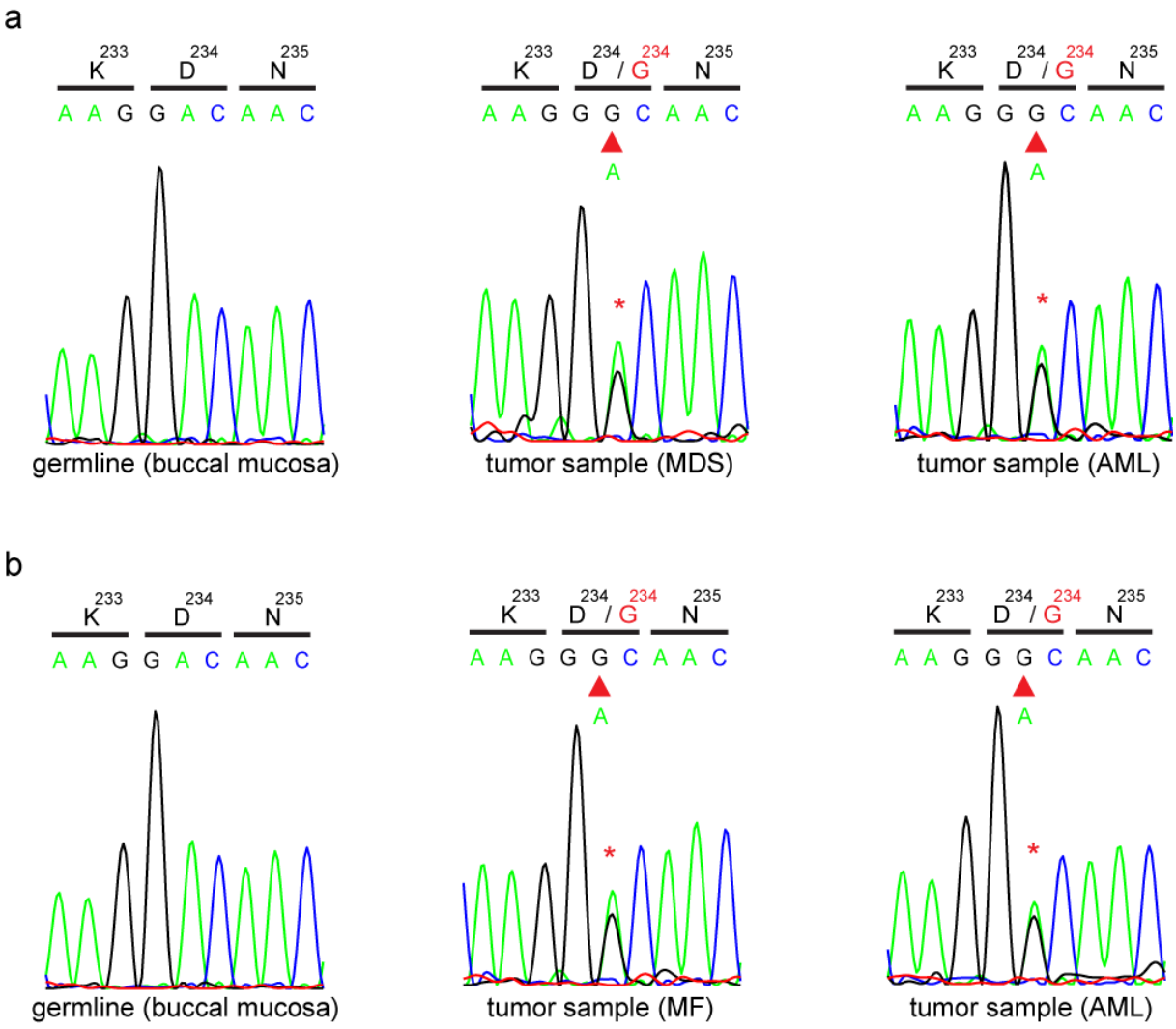

Figure 5.
***CDC25C* mutations validated by Sanger sequencing.** The result of Sanger sequencing for the *CDC25C* mutations found in whole-exome sequencing is shown. Both forward and reverse traces were available for each mutation but only one trace is shown above. The results of buccal mucosa, pre-leukemic phase, and leukemic phase is demonstrated in Subject 20 (**a**) and Subject 21 (**b**), respectively.

Clonal evolution model of FPA/AML derived AML

We next unmasked the details of clonal evolution and expansion leading to AML through the use of deep sequencing of individual mutations detected by whole-exome sequencing. Intratumoral heterogeneity was evident at both MDS phase and AML phase in Subject 20 (**Fig. 6b**). According to the predicted model, a founder clone with *CDC25C* mutation acquired *COL9A1*, *FAM22G*, and *LPP* mutations (group 1), and subsequent emergence of *GATA2* mutation (group 2) triggers full-blown leukemia, whereas another subclone defined by *CHEK2* and other mutations in 3 genes (group 3) relatively regressed. To validate this hierarchical model, single cell genomic sequencing was performed using genome DNA of 63 bone marrow cells from Subject 20 at the AML phase. Based on the ratio of *RUNX1* mutation in these cells, false negative rate of the procedure was relatively high as estimated to be 35 %, possibly due to biased allele amplification. However, this technique succeeded in demonstrating that group 1/2 and group 3 mutations were mutually exclusive (**Fig. 6c and Table 6**). Similarly, genetic architecture was depicted for Subject 21 (**Fig. 6d**). In both scenarios, *CDC25C* mutations showed higher allele frequencies than did the mutations in the other groups, suggesting that *CDC25C* mutation contributed to the establishment of founding tumor population as an early genetic event, whereas progression to AML seemed to be accompanied by additional mutations, indicating a multistep process of leukemogenesis.

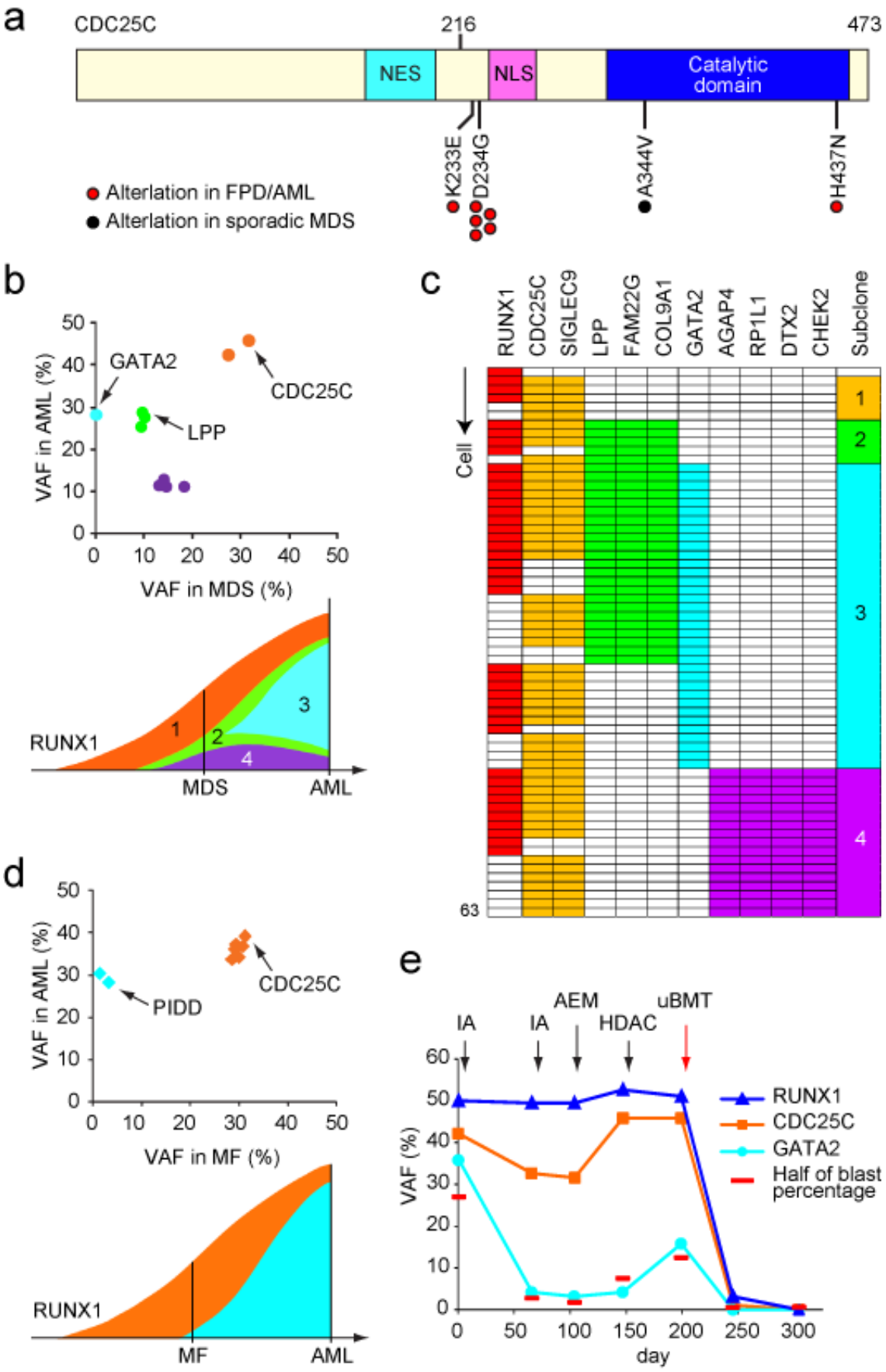
a
CDC25C
216
473
NES
NLS
Catalytic domain
K233E
D234G
A344V
H437N
Alterlation in FPD/AML
Alterlation in sporadic MDS
b
VAF in AML (%)
VAF in MDS (%)
GATA2
CDC25C
LPP
RUNX1
MDS
AML
c
RUNX1
CDC25C
SIGLEC9
LPP
FAM22G
COL9A1
GATA2
AGAP4
RP1L1
DTX2
CHEK2
Subclone
Cell
63
d
VAF in AML (%)
VAF in MF (%)
PIDD
CDC25C
RUNX1
MF
AML
e
IA
IA
AEM
HDAC
uBMT
VAF (%)
day
RUNX1
CDC25C
GATA2
Half of blast percentage

Figure 6.

***CDC25C* mutation forms founding malignant clone in the clonal evolution of FPD/AML.** (**a**) The distribution of alterations is shown for CDC25C protein. NES, a putative nuclear export signal domain between amino acids 177-200; NLS, a putative nuclear localization sequence domain consisting of amino acids 240-244. (**b**) Observed variant allele frequency (VAF) of validated mutations listed in **Table 2** in both pre-leukemic and leukemic phases are shown in diagonal plots (top) for Subject 20. Predicted chronological behaviors in different leukemia subclones are depicted below each diagonal plot. Distinct mutation clusters are displayed by color. VAF of *CDC25C* mutation was the highest among that of other genes at both pre-leukemic and leukemic phase, suggesting that *CDC25C* mutation is an early event during the transformation of FPD/AML and establishes founding malignant clone. (**c**) The mutation status of each bone marrow cell from Subject 20 at AML phase which was full of blasts. The vertical axis represents each cell (n=63) and the horizontal axis displays each gene mutation. Colored columns show that the corresponding cell harbors gene mutation(s) as defined in methods. Subclone numbers shown in the right row corresponds to the numbers in the lower figure of **Fig. 6b**. (**e**) VAFs of *RUNX1*, *CDC25C*, and *GATA2* mutation are demonstrated with the time course of treatment. Half the value of the blast percentage, which corresponds to the allele frequency of a heterozygous mutation, is also shown by a red bar. IA, idarubicine + Ara-C; AEM, Ara-C + etoposide + mitoxantrone; HDAC, High dose Ara-C; uBMT, unrelated bone marrow transplantation.

Table 6. Mutational status of each bone marrow cell from Subject 20 at AML phase

Cell	RUNX1	CDC25C	SIGLEC9	group 1			group 2	group3				Clone
				LPP	FAM22G	COL9A1	GATA2	AGAP4	RP1L1	DTX2	CHEK2	
8	Mutation+	-	-	x	-	x	x	x	x	x	-	0
4	Mutation+	Mutation+	Mutation+	x	x	x	-	-	x	x	x	1
22	Mutation+	Mutation+	x	-	x	x	-	x	x	x	-	1
32	Mutation+	Mutation+	-	x	x	-	-	-	x	x	-	1
19	-	Mutation+	-	x	-	x	x	-	x	x	x	1
34	x	Mutation+	-	-	x	x	x	-	x	x	-	1
12	Mutation+	Mutation+	-	Mutation+	Mutation+	x	-	x	-	x	x	2
13	Mutation+	Mutation+	Mutation+	-	x	Mutation+	-	x	x	x	-	2
60	Mutation+	Mutation+	-	x	-	Mutation+	-	-	-	x	-	2
1	Mutation+	-	x	-	Mutation+	x	-	-	-	x	-	2
24	-	Mutation+	x	Mutation+	Mutation+	x	x	x	x	x	x	2
6	Mutation+	Mutation+	-	Mutation+	-	Mutation+	Mutation+	-	-	x	-	3
18	Mutation+	Mutation+	x	-	x	Mutation+	Mutation+	-	-	x	-	3
21	Mutation+	Mutation+	-	-	Mutation+	x	Mutation+	-	x	x	-	3
26	Mutation+	-	Mutation+	Mutation+	Mutation+	Mutation+	Mutation+	-	x	x	-	3
38	Mutation+	x	Mutation+	Mutation+	-	Mutation+	Mutation+	-	x	x	-	3
47	Mutation+	Mutation+	-	Mutation+	x	Mutation+	Mutation+	-	-	x	-	3
49	Mutation+	Mutation+	-	Mutation+	Mutation+	-	Mutation+	-	-	x	-	3
58	Mutation+	-	Mutation+	Mutation+	-	Mutation+	Mutation+	-	-	-	-	3
63	Mutation+	Mutation+	Mutation+	Mutation+	x	Mutation+	Mutation+	-	-	-	-	3
64	Mutation+	-	Mutation+	-	-	Mutation+	Mutation+	-	-	-	-	3
9	Mutation+	Mutation+	Mutation+	Mutation+	x	-	Mutation+	-	x	x	-	3
3	Mutation+	-	x	-	Mutation+	x	Mutation+	x	-	-	-	3
17	Mutation+	-	x	-	Mutation+	x	Mutation+	-	x	x	-	3
35	Mutation+	-	-	Mutation+	Mutation+	x	Mutation+	-	-	x	-	3
37	Mutation+	-	-	Mutation+	x	Mutation+	Mutation+	-	-	x	-	3
2	-	Mutation+	x	Mutation+	Mutation+	x	Mutation+	-	-	x	-	3
27	-	-	Mutation+	-	x	Mutation+	Mutation+	-	x	x	x	3
30	-	Mutation+	-	-	x	Mutation+	Mutation+	-	x	x	x	3
48	-	Mutation+	x	Mutation+	Mutation+	x	Mutation+	-	-	x	x	3
51	-	Mutation+	-	-	Mutation+	Mutation+	Mutation+	-	-	x	-	3
61	-	Mutation+	x	Mutation+	x	x	Mutation+	-	x	x	-	3
14	-	-	-	-	Mutation+	x	Mutation+	-	-	x	-	3
41	-	-	-	-	x	Mutation+	Mutation+	-	x	x	x	3
39	Mutation+	Mutation+	-	-	-	-	Mutation+	-	x	x	-	3
40	Mutation+	Mutation+	-	-	-	-	Mutation+	-	x	x	-	3
45	Mutation+	Mutation+	-	-	x	x	Mutation+	-	x	x	-	3
46	Mutation+	Mutation+	x	-	-	x	Mutation+	x	x	x	-	3
53	Mutation+	-	Mutation+	-	x	-	Mutation+	-	-	x	-	3
56	Mutation+	Mutation+	Mutation+	-	x	x	Mutation+	x	x	x	x	3
62	Mutation+	-	Mutation+	-	x	x	Mutation+	-	-	-	-	3
5	Mutation+	-	-	-	-	-	Mutation+	-	-	x	-	3
28	x	-	Mutation+	-	-	x	Mutation+	-	x	x	x	3
42	-	Mutation+	Mutation+	-	x	x	Mutation+	-	x	x	x	3
50	-	Mutation+	-	-	x	-	Mutation+	-	x	-	-	3
55	-	Mutation+	-	-	x	x	Mutation+	-	x	-	-	3
15	Mutation+	Mutation+	-	-	x	-	-	Mutation+	x	Mutation+	x	4
20	Mutation+	Mutation+	-	-	-	-	-	-	Mutation+	x	x	4
31	Mutation+	Mutation+	-	-	x	x	-	-	Mutation+	x	x	4
36	Mutation+	Mutation+	Mutation+	-	-	x	x	-	Mutation+	x	x	4
43	Mutation+	Mutation+	Mutation+	-	-	-	-	Mutation+	x	Mutation+	-	4
54	Mutation+	Mutation+	-	-	x	x	-	Mutation+	Mutation+	x	-	4
57	Mutation+	Mutation+	-	x	x	x	x	Mutation+	-	x	-	4
59	Mutation+	Mutation+	-	x	-	-	-	-	Mutation+	x	-	4
10	Mutation+	-	-	-	-	-	-	-	-	Mutation+	-	4
11	Mutation+	-	-	-	-	-	-	Mutation+	Mutation+	x	x	4
7	-	Mutation+	-	x	-	x	x	Mutation+	x	x	Mutation+	4
16	-	Mutation+	x	-	x	-	-	Mutation+	Mutation+	x	-	4
23	-	Mutation+	-	x	-	x	x	Mutation+	-	x	x	4
25	-	Mutation+	-	x	x	x	-	x	Mutation+	Mutation+	x	4
29	-	-	Mutation+	-	x	-	-	Mutation+	x	Mutation+	-	4
33	-	Mutation+	Mutation+	-	-	x	x	x	Mutation+	x	Mutation+	4
52	x	-	Mutation+	x	-	-	-	Mutation+	-	Mutation+	Mutation+	4
								-, mutation not detected; x, undetermined				

Definition of the clone 1-4

RUNX1	CDC25C	SIGLEC9	LPP	FAM22G	COL9A1	GATA2	AGAP4	RP1L1	DTX2	CHEK2	clone
Mutation+											0
Mutation+	Mutation+	Mutation+									1
Mutation+	Mutation+	Mutation+	Mutation+	Mutation+	Mutation+						2
Mutation+	Mutation+	Mutation+	Mutation+	Mutation+	Mutation+	Mutation+					3
Mutation+	Mutation+	Mutation+					Mutation+	Mutation+	Mutation+	Mutation+	4

VAFs of *CDC25C* and *GATA2* corresponding to the clinical course

Among the somatic mutations found in Subject 20 and 21, *GATA2* mutation was also identified in Subject 22 (**Fig. 7a**). This patient developed AML with multilineage dysplasia, leading to the diagnosis of AML-MRC. Remission induction therapies were partially effective and the blast ratio was reduced from 54 % to 5.6 %, while dysplastic feature persisted (**Fig. 6e** and **Fig. 7b**). Allogeneic stem cell transplantation was successfully performed from an HLA-matched unrelated donor and complete remission with 100 % donor chimerism was obtained. During the treatment, variant allele frequency (VAF) of *GATA2* mutation decreased almost in parallel with blast percentage while VAF of *CDC25C* mutation hovered at a high ratio before transplantation, suggesting that *GATA2* mutation confers leukemia progression in this patient whereas *CDC25C* mutation is associated with pre-leukemic status. Another type of *GATA2* mutation was found in Subject 18 with allelic frequency of 0.94 %, who showed thrombocytopenia but have a small clone with *CDC25C* mutation at the same time (**Fig. 7c**). Further sequence analysis in 90 sporadic MDS patients and 53 AML patients identified only one CDC25C mutation (p.Ala344Val) in a MDS patient among 13 MDS patients with *RUNX1* mutation (**Fig. 8 and Table 7**).

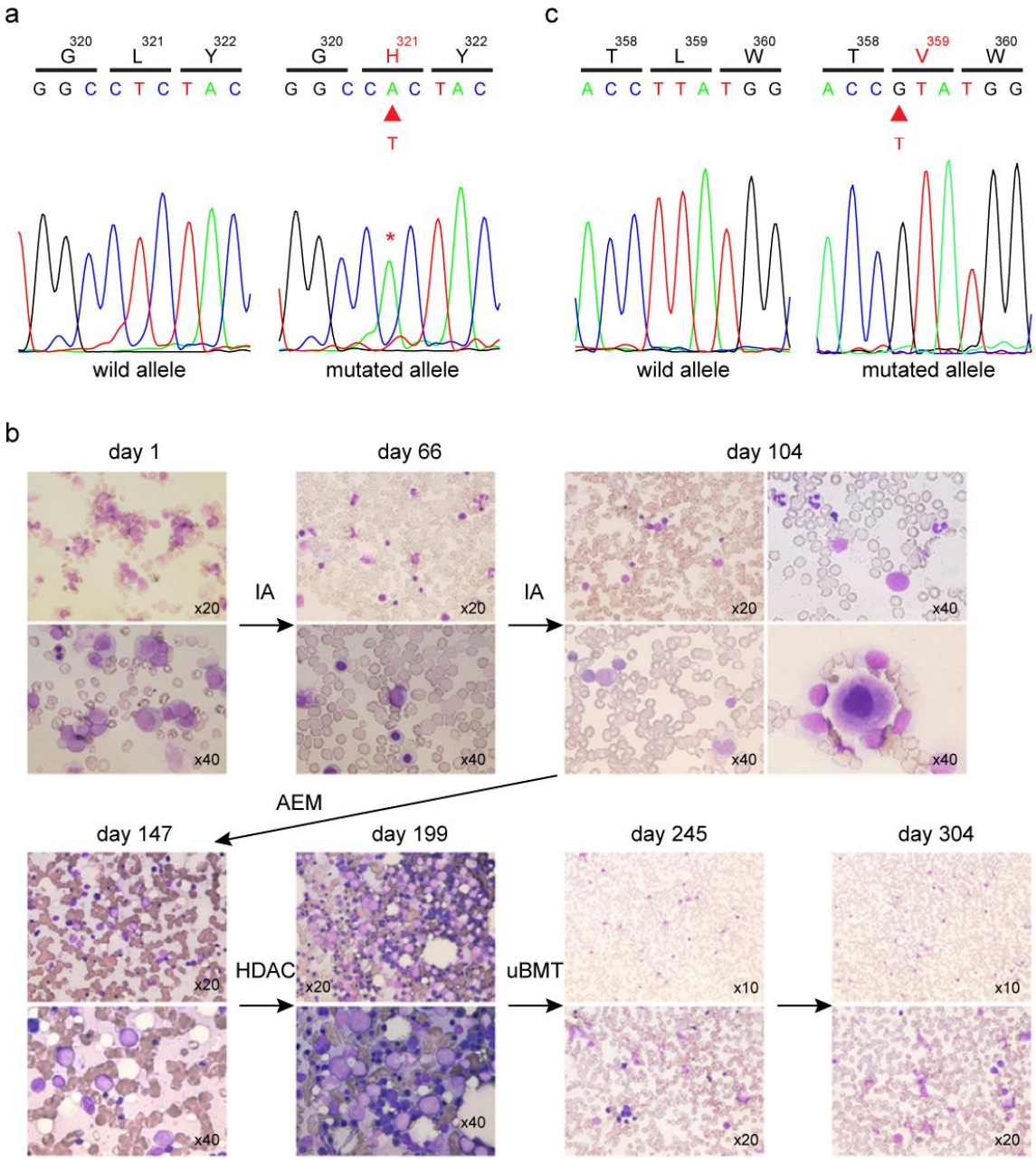

Figure 7.

***GATA2* mutations and the bone marrow smears of Subject 22.** (**a,c**) The result of Sanger sequencing for GATA2_p.Leu321His (**a**) and p.Leu359Val (**c**) mutations validated with subcloning strategy. (**b**) Smears of the bone marrow are shown with the time course of treatment. The blast percentage was decreased with induction therapy. However, dysplastic features such as degranulation of neutrophil and micromegakaryocytes / mononucleated megakaryocytes were evident on day 104, suggesting a pathological condition similar to MDS. Although we changed the chemotherapeutic agents, they were not effective and the bone marrow became hyperplastic. As the bone marrow aspirates were dry tap, stamp preparations with her bone marrow biopsy were shown on day 147 and day 199. She received BMT from an HLA-matched unrelated donor with conditioning with cyclophosphamide 120 mg/mg + 12 Gy of total body irradiation on day 215. Engraftment was obtained on day 241 (26 days after BMT) and she is in excellent health and free from relapse on day 2259 (2044 days after BMT).

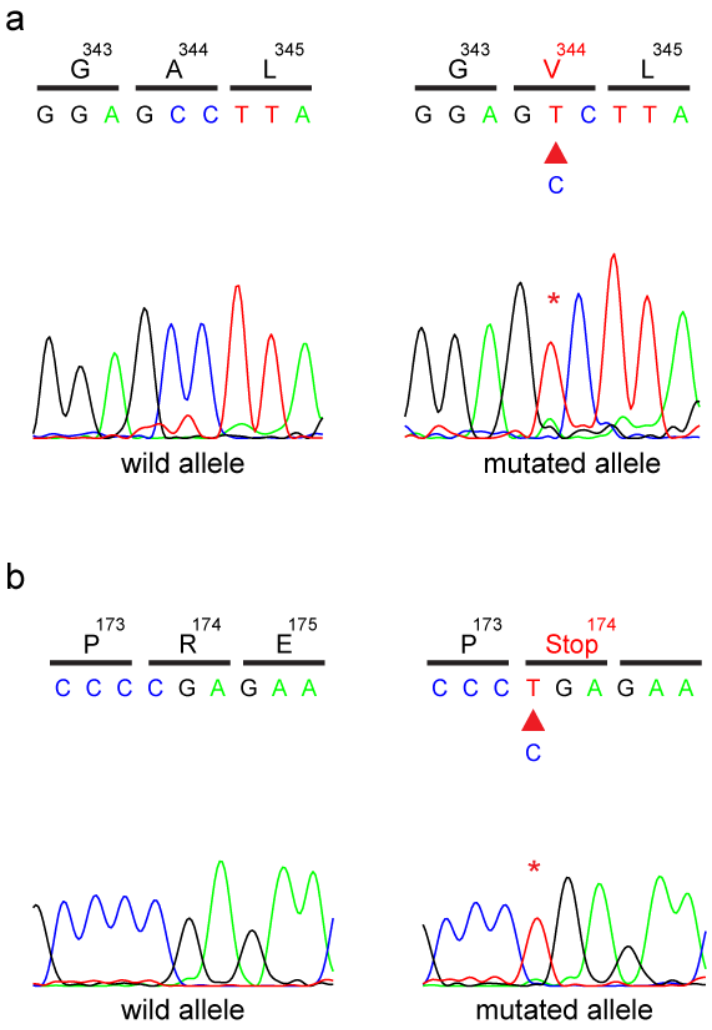

Figure 8. Co-existence of *CDC25C* and *RUNX1* mutations in a sporadic MDS patient. The result of Sanger sequencing for the *CDC25C*_p.Ala344Val (**a**) and *RUNX1*_p.Arg174* (**b**) mutations validated with subcloning strategy.

Table 7. Mutational status of *CDC25C and RUNX1* in sporadic MDS and AML patients.

		CDC25C mutation	
MDS (n=90)		+	-
RUNX1 mutation	+	1	12
	-	0	77
AML (n=53)		+	-
RUNX1 mutation	+	0	3
	-	0	50

Disruption of G2/M checkpoint by CDC25C mutants

We next investigated the possible impact of *CDC25C* mutation because it is still unclear whether *CDC25C* represents a new recurrent mutational target in human cancer. CDC25C is a phosphatase that prevents premature mitosis in response to DNA damage at the G2/M checkpoint, while it is constitutively phosphorylated at p.Ser216 throughout the interphase by c-TAK1[15-17]. When phosphorylated at Ser216, CDC25C binds to 14-3-3 protein[18], which sequestrates CDC25C in the cytoplasm and inactivates it. Ba/F3 cells were transduced with retroviruses encoding wild-type or mutant (p.Asp234Gly, p.Ala344Val, p.His437Asn, p.Ser216Ala) CDC25C and assayed. P.Ser216Ala mutant form was used as a negative control lacking the phosphorylation site. In all of the mutated forms of CDC25C, their binding capacity with c-TAK1 was reduced (**Fig. 9a**), resulting in decreased phosphorylation status of CDC25C at p.Ser216 (**Fig. 9b**). As a consequence, mutated CDC25C failed to bind with 14-3-3 protein efficiently (**Fig.9c**) and stayed in the nucleus even though cell synchronization was achieved at the G1/S phase by treatment with thymidine (**Fig. 9d and Fig. 10**). In accordance with these observations, CDC25C mutants led to enhanced mitosis entry (**Fig. 11**), which was exaggerated by low dose radiation-induced DNA damage (**Fig. 9e**). These results suggest that *CDC25C* mutation results in disruption of DNA checkpoint machinery and accelerates genomic instability.

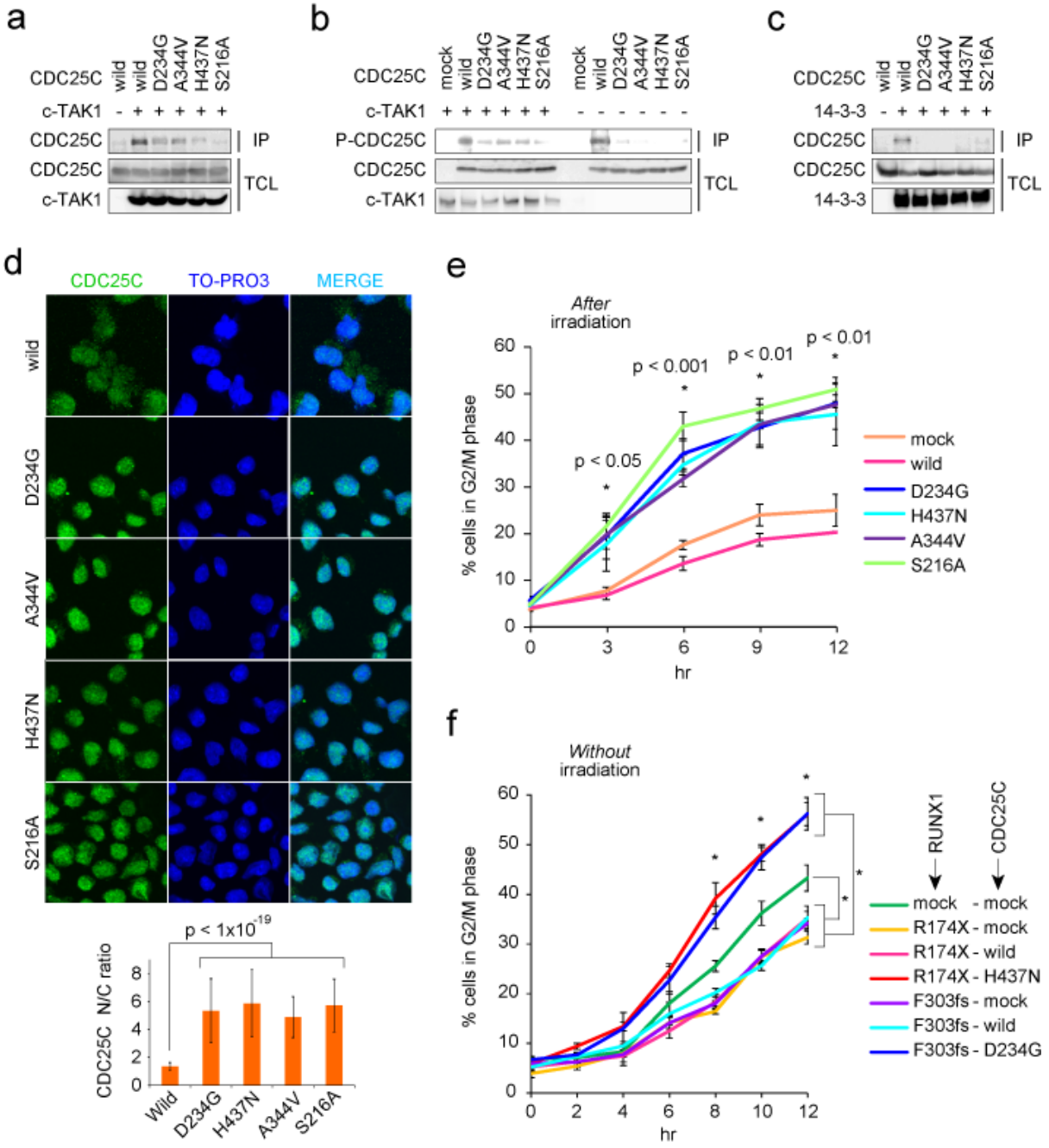

Figure 9.

Mutated CDC25C enhances mitosis entry. (**a**) HEK293T cells were transiently transfected with Flag-tagged CDC25C or its mutant and HA-tagged c-TAK1 as indicated and cell lysates were immunoprecipitated with anti-HA antibody. Binding capacity of CDC25C was evaluated by western blotting. IP, immunoprecipitation; TCL, total cell lysate. (**b**) Cell lysates were prepared as shown above and immunoprecipitated with anti-Flag (CDC25C) antibody. Phosphorylation levels of CDC25C were visualized by phosphorylated-Ser216 specific anti-CDC25C antibody. (**c**) Mutated CDC25C shows reduced binding capacity with 14-3-3. Experiments were performed using a plasmid encoding HA-tagged 14-3-3. (**d**) Localization of CDC25C or its mutants were visualized by immunofluorescence. N/C ratio of each cell was calculated as detailed in methods and **Fig.10**. The average N/C ratio with SD was presented. The significance of difference was determined by unpaired Student *t* test (n > 50 for each). (**e**)

Mitosis entry of CDC25C-mutated cells after 2 Gy of irradiation was analyzed over time as described in methods and **Fig. 11a**. Percentage of mutated CDC25Cs-tansduced cells in G2/M phase was compared with that of wild-type CDC25C-transduced cells. P values were calculated by Student *t* test and maximal p value among these comparisons were shown at each time point (n=3). (**f**) RUNX1 and CDC25C mutation are co-expressed in Ba/F3 cells as indicated and mitosis entry of these cells was evaluated. The differences between groups as indicated were all statistically significant (*p <0.01) at 8, 10, and 12 hrs after washout of thymidine (n=3). P values were determined by Student *t* test.

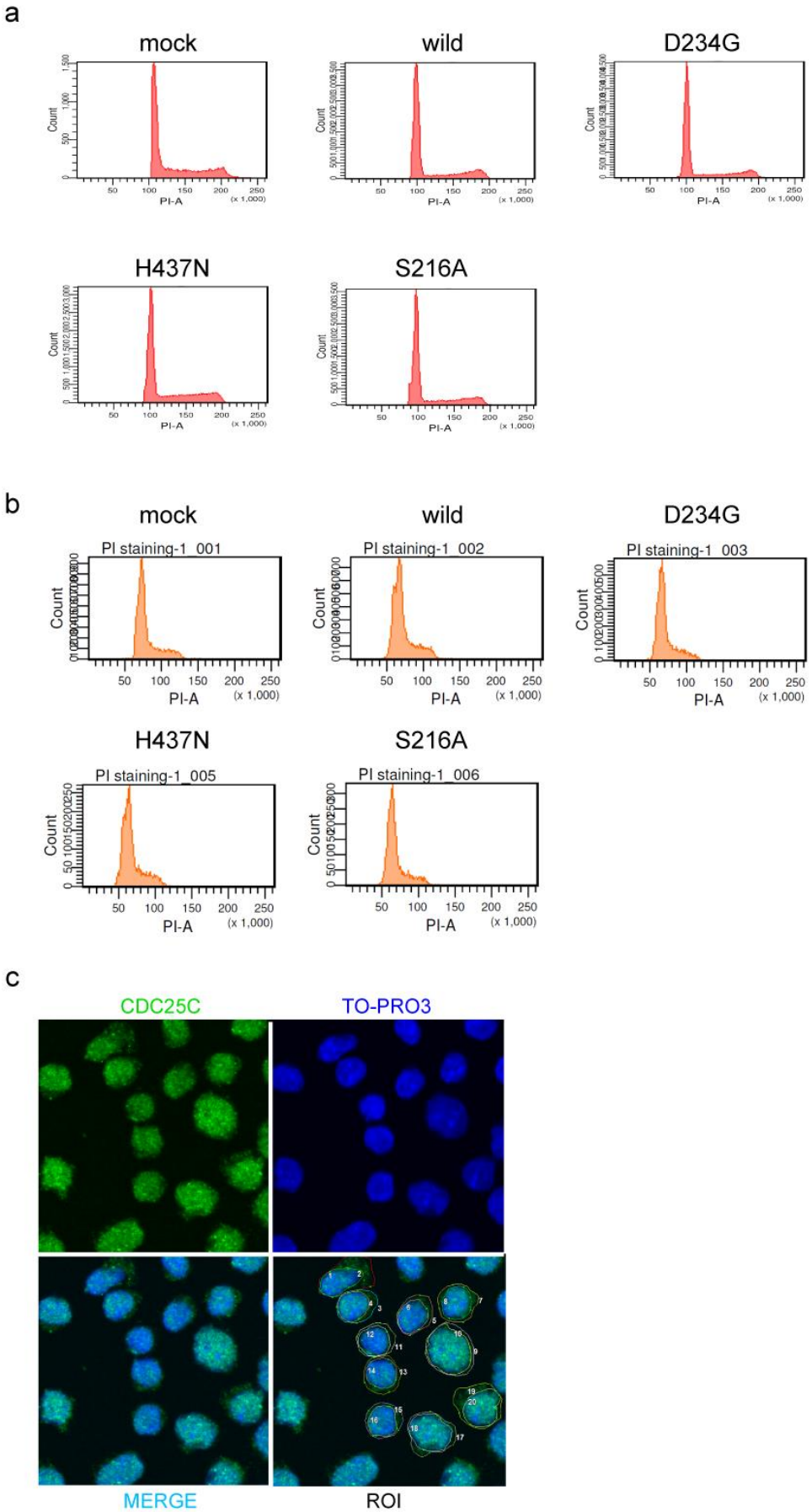
a
mock
wild
D234G
H437N
S216A
Count
PI-A
(x 1,000)
b
mock
wild
D234G
H437N
S216A
PI staining-1_001
PI staining-1_002
PI staining-1_003
PI staining-1_005
PI staining-1_006
Count
PI-A
(x 1,000)
c
CDC25C
TO-PRO3
MERGE
ROI

Figure 10.

Estimation of CDC25C localization based on immunofluorescence. (**a, b**) Cell cycle was evaluated by PI staining (a) in a steady state or (b) after treatment with thymidine for 12 hrs and cell synchronization was achieved. Representative figures are shown. (**c**) Localization of CDC25C or its mutants were visualized by immunofluorescence. The mean intensity of CDC25C in nucleus and cytoplasm of each cell was measured within a region of interest (ROI) placed within nucleus and cytoplasm. Similarly, the background intensity was quantified within ROI placed outside the cells. All the measurements were performed using the Fluoview software. The background-subtracted intensity ratio of nucleus to cytoplasm was calculated in more than 50 cells in each specimen and the average intensity with SD was presented. A representative figure of ROI placed on 10 cells is shown.

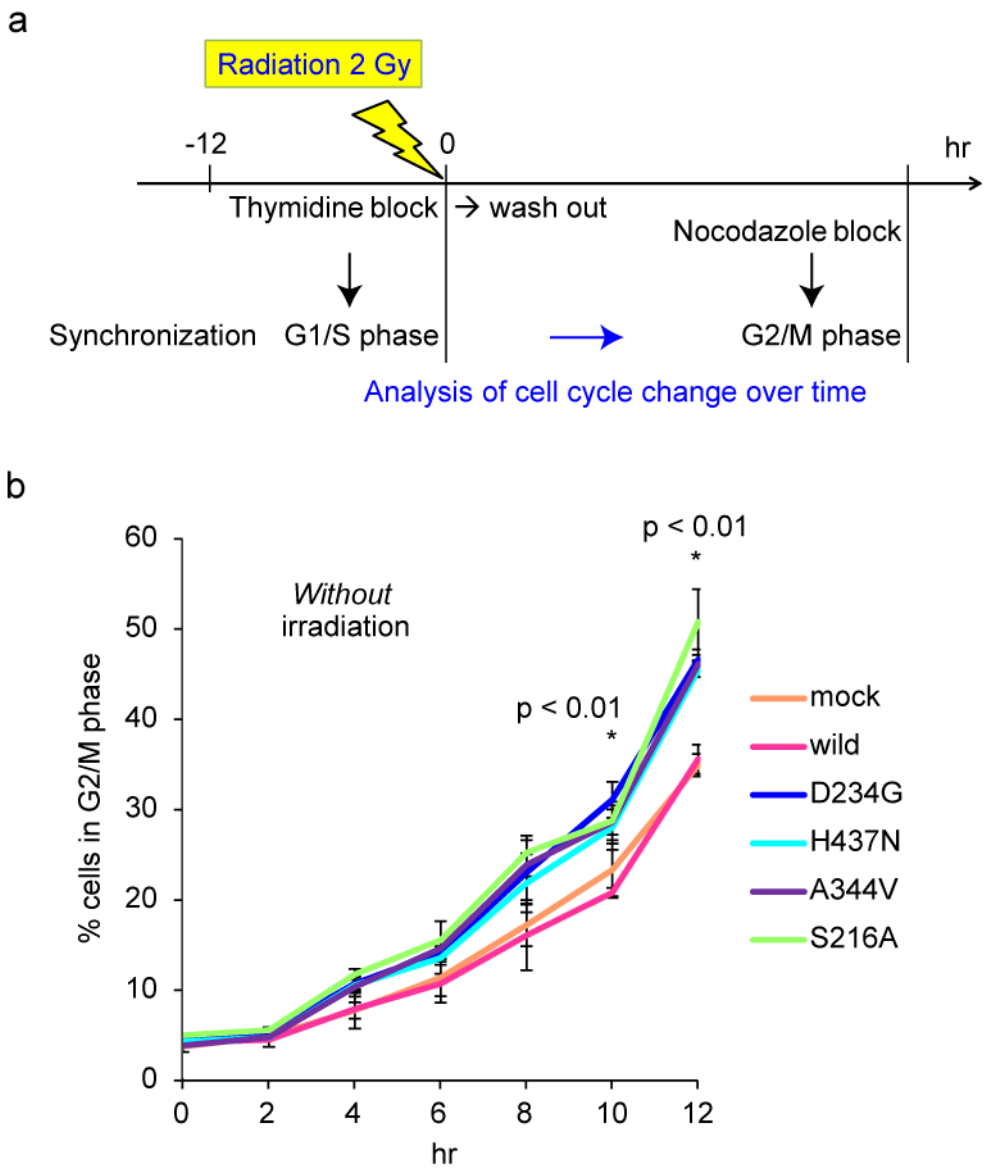

Figure 11. Analysis of mitosis entry in CDC25C mutated cells. (**a**) Schematic description of the method used for evaluation of mitosis entry. After cell synchronization using thymidine for 12 hrs, thymidine was washed out and the cells were irradiated and incubated with nocodazole. Cell cycle was analyzed over time by PI staining. (**b**) Mitosis entry of CDC25C-mutated cells was analyzed as **Fig. 9e**. Cell cycle was analyzed over time as indicated. Percentage of mutated CDC25Cs-tansduced cells in G2/M phase was compared with that of wild-type CDC25C-transduced cells. The significance of difference was determined by Student *t* test and maximal p values among these comparisons were shown at each time point (n=3). Error bars represent SD.

Oncogenic cooperation of *RUNX1* and *CDC25C*

Next we asked why *CDC25C* abnormality is a frequent genetic event in FPD/AML. It is known that *RUNX1* mutations evoke DNA damage and subsequent cell cycle arrest in hematopoietic cells[19,20]. We confirmed that FPD/AML-associated *RUNX1* mutations also induce DNA damage through transcriptional suppression of several genes involved in DNA repair (**Fig. 12**), with activation of the G2/M checkpoint mechanism in the presence of *RUNX1* mutations (**Fig. 9f**). We found, however, that introduction of *CDC25C* mutation resulted in enhancement of mitosis entry in spite of co-existence of *RUNX1* mutations (**Fig. 9f**). Therefore, premature mitosis by deregulated DNA checkpoint mechanisms evoked by *CDC25C* mutation may contribute to malignant transformation in concert with the DNA damage derived from *RUNX1*-mutation.

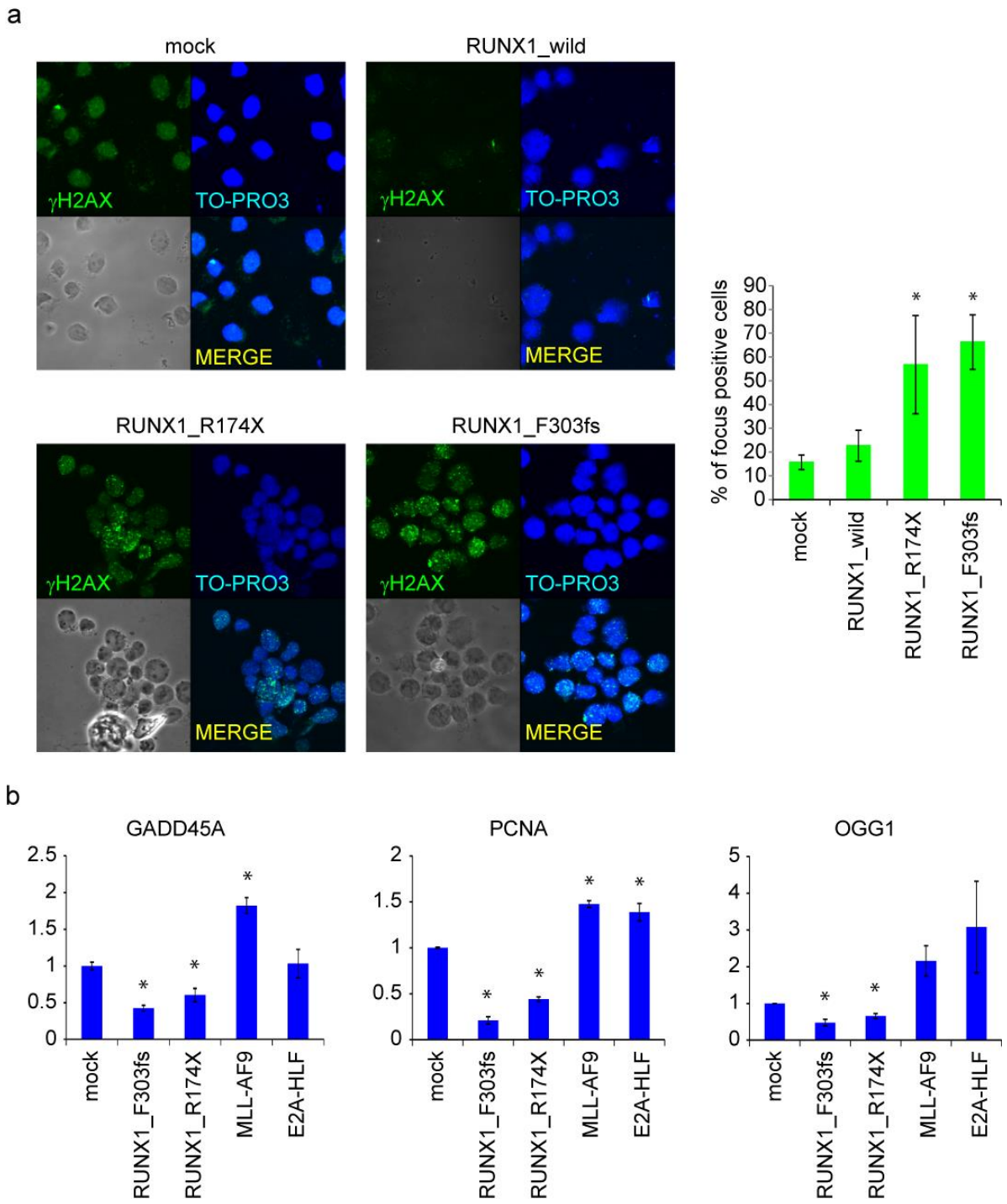

Figure 12.

RUNX1 mutations induce DNA damage via suppression of DNA repair genes. (**a**) Ba/F3 cells transduced with RUNX1 mutations show enhanced DNA damage as depicted by increased γH2AX foci. Representative figures are shown in the left. The right graph demonstrates percentage of γH2AX focus positive cells in 100 cells. Asterisks represent statistically significant difference compared with wild-type RUNX1-transduced cells (*$p < 0.05$). Error bars represent SD. (**b**) Results of qPCR for GADD45A, PCNA, and OGG1 in Ba/F3 cells transduced with indicated oncogenes are demonstrated, respectively. The results were normalized to 18s ribosomal RNA level. Asterisks represent statistically significant difference compared with mock-transduced cells (*$p < 0.01$). Error bars represent SD.

Discussion

In this study, we identified *CDC25C* as a new recurrent mutational target in FPD/AML using next-generation sequencing and showed that *RUNX1* mutation and *CDC25C* mutation collaboratively induce cell cycle progression under DNA damage. FPD/AML hematopoietic cells were shown to acquire *CDC25C* mutations initially, accumulate additional mutations such as *GATA2*, and finally develop into hematological malignancy.

For Subject 20, variant allele frequency of SIGLEC9_p.Ser437Gly was approximately as high as that of CDC25C_p.Asp234Gly at MDS and AML phase. However, only one SIGLEC9 isoform (isoform 1) has p.Ser437 locus and we could only recognize the expression of another isoform (isoform 2) for some human leukemic cell lines (data not shown). Therefore, we considered the expression of SIGLEC9 in leukemic cells was mostly restricted to isoform 2 and SIGLEC9_p.Ser437 mutation hardly seemed to have functional impact in leukemogenic process.

To our knowledge, this nationwide survey is the largest study to investigate the pedigrees with FPD/AML. We detected 7 pedigrees with germline *RUNX1* mutation, and 7 out of 13 patients (53.8 %) in these pedigrees had developed hematological malignancies. The frequency of hematological malignancies in FPD/AML pedigrees was comparable to the previous reports[21]. In our survey, there was no statistically significant difference in clinical features and complete blood count between FPD/AML and non-FPD/AML patients. In addition, thrombocytopenia was sometimes absent in patients with inherited *RUNX1* mutation, and FPD/AML patients without thrombocytopenia can later suffer from hematological malignancy. As it seems hard for clinicians to distinguish FPD/AML patients from non-FPD/AML patients in daily practice, we should analyze *RUNX1* mutation status in patients with familial hematological disorders.

We also detected 2 pedigrees with germline *MYH9* mutation. May-Hegglin anormaly, also called *MYH9*-related disease, is a rare autosomal dominant disorder caused by inherited *MYH9* mutation and characterized by macrothrombocytopenia, giant platelet, leukocyte inclusion, deafness, nephritis and/or cataract[22]. Many loss-of-function point mutations were reported about *MYH9* and Asp1424 is a relatively common mutation site. Phe41 mutation, which has never been reported, is a change in the globular head domain in MYH9 and may influence the ability to hydrolyze ATP and slide along actin filament. Meanwhile, no responsible germline mutation was detected in other 36 pedigrees with familial thrombocytopenia or hematological malignancy. Some pedigrees with strong family histories may harbor unknown inherited leukemogenic mutation other than *RUNX1* or other genes investigated in this survey. Further study is warranted in this point.

Treatment strategy for hematological malignancies from FPD/AML has not been established yet. Considering the increased efficacy of PARP inhibitor against familial breast cancer with BRCA mutation[23], impaired DNA damage response (DDR) in FPD/AML leukemic cells also can be an attractive treatment target of DDR-directed agents such as PARP inhibitors. However, we should consider that normal hematopoietic cells of FPD/AML patients also harbor *RUNX1* mutation with potential genomic instability. Cytotoxic drugs or other DNA damaging agents might cause extensive mutations in non-leukemic cells and induce second malignancies. Allogeneic stem cell transplantation might be one of the reasonable treatment choices as seen in clinical history of Subject 22, although further investigations are warranted.

In the previous reports about *RUNX1* mutation, pathogenicity of RUNX1 mutations was mainly linked with differentiation block or increased self-renewal capacity[11]. However, as RUNX1_p.Phe303fs and RUNX1_p.Arg174X disrupt DDR, life-long genomic instability

may have an important role in tumor development in FPD/AML patients and the mutagenicity induced by RUNX1 mutations is exaggerated by CDC25C alteration as we disclosed above.

These results provide a detailed look at genetic landscape of FPD/AML and how these mutations can drive malignant transformation. In particular, the high frequency of *CDC25C* mutation in FPD/AML (46 %) underscores a major role in the pathogenesis of FPD/AML. Evaluation of the allelic burden of mutated genes highlighted a hierarchical model and clonal selection in which *CDC25C* mutation recurrently preceded subclonal mutations in *GATA2* and other genes. Considering that *CDC25C* mutation is an initial event during the malignant transformation and that a small clone with *CDC25C* mutation can be detected in FPD/AML patients without clinically apparent malignancy, examination in the allelic burden of *CDC25C* mutation may mark patients at risk for the development of malignancy. Although precise pathogenetic roles of mechanisms of *CDC25C* mutations are still unclear, we have shown that mutant *CDC25C* alleles confer advantage for proliferation under certain circumstance with increased DNA damage. It remains to be elucidated why *CDC25C* mutations are repetitively documented in FPD/AML but not in sporadic MDS or AML. As the phenotypes of CDC25C-mutated cells are significant but not so extensive, it could take relatively long latency for these cells to gain further oncogenic abnormality and some cooperative carcinogen with high compatibility such as *RUNX1* mutations might be necessary to exert oncogenic capacity of *CDC25C* mutations. These results might be in agreement with the clinical findings that approximately 40 % of patients with FPD/AML develop leukemia in their thirties. Among the patients with *CDC25C* mutations in FPD/AML, mutations in *GATA2* are identified in 3 out of 7 patients (Subject 18, 20, and 22). Although the reports on clinical relevance of *GATA2* mutation in myeloid malignancy are limited, several lines of evidence

have recently been reported. *GATA2* mutation is frequently found in a subgroup with biallelic *CEBPA* gene mutations in cytogenetically normal AML[24], which account for about 4 % of AML. Mutation in *GATA2* is also observed in disorders linked to an increased predisposition to develop MDS/AML such as Emberger syndrome, MonoMAC syndrome and DCML deficiency[25-27]. The position of p.Leu321His and p.Leu359Val, which are found in FPD/AML patients, are located at the N-terminal and C-terminal zinc finger domain of GATA2, respectively (**Fig. 13a**) and alterations at the identical amino acid have been reported in AML with *CEBPA* mutation and chronic myeloid leukemia in blast crisis[24,28]. Thus *GATA2* mutation might contribute to AML progression in collaboration with *RUNX1* and/or *CDC25C* alteration.

In conclusion, FPD/AML-associated malignant transformation is formed by stepwise acquisition of mutations and clonal selection, which is initiated by a *CDC25C* mutation in the pre-leukemic phase and further driven by mutations in *GATA2* or other genes (**Fig. 13b**). The identification of *CDC25C* as the gene responsible for the transformation will facilitate the diagnosis and monitoring of individuals with FPD/AML who are at an increased risk of developing life-threatening hematological malignancy.

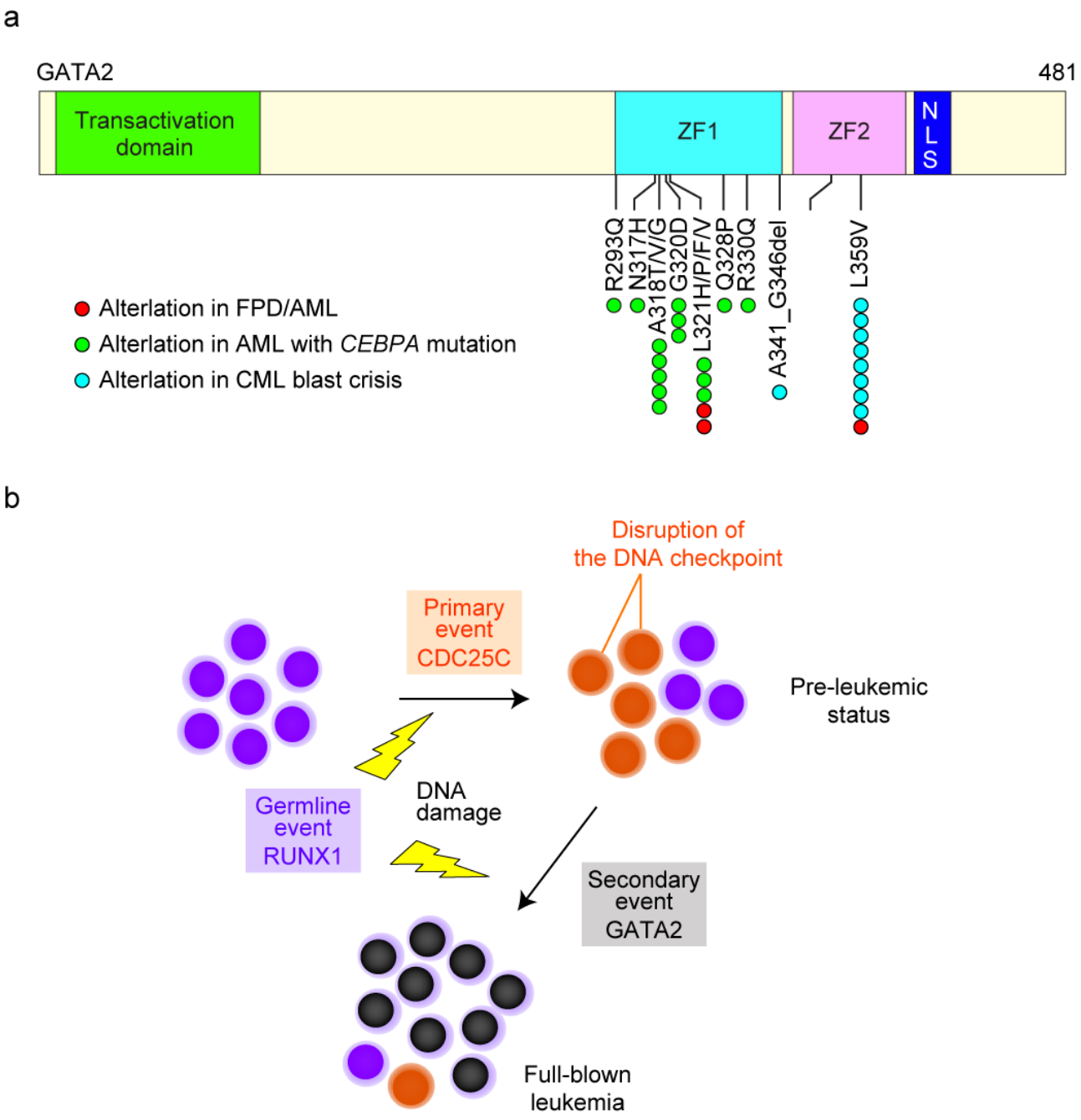

Figure 13.

Secondary genetic event in FPD/AML. (**a**) Schematic representation of *GATA2* mutations. GATA2 mutations that were identified in FPD/AML are displayed together with mutations found in AML with CEBPA mutation[24] and in CML blast crisis[28]. ZF, zinc finger domain; NLS, a putative nuclear localization sequence domain. (**b**) Clonal history of gene mutations in FPD/AML.

URLs.

dbSNP, http://www.ncbi.nlm.nih.gov/projects/SNP/;

the 1000 Genomes Project, http://www.1000genomes.org/;

the UCSC Genome Browser, http://genome.ucsc.edu/cgi-bin/hgGateway/;

hg19, http://hgdownload.cse.ucsc.edu/goldenPath/hg19/database/;

RefSeq genes, http://www.ncbi.nlm.nih.gov/RefSeq/;

SIFT, http://sift.jcvi.org/;

PolyPhen-2, http://genetics.bwh.harvard.edu/pph2/.

Acknowledgements

I would like to express my sincere gratitude to my supervisor, Professor Mineo Kurokawa for providing me this precious study opportunity as a Ph.D student in his laboratory. I especially would like to express my deepest appreciation to my supervisor, Dr. Akihide Yoshimi for his elaborated guidance, considerable encouragement and invaluable discussion that make my research of great achievement and my study life unforgettable. I am very grateful to Masahiro Nakagawa, Masahito Kawazu, Shunya Arai, Motoshi Ichikawa, Hironori Harada, Kensuke Usuki, Yasuhide Hayashi, Etsuro Ito, Keita Kirito, Hideaki Nakajima, Hiroyuki Mano for their valuable cooperation in my experiments.

We thank R. Lewis (University of Nebraska Medical Center) for providing materials. T.Koike (Nagaoka Red Cross Hospital), K. Nara (Ootemachi Hospital), K. Suzuki (Japanese Red Cross Medical Center), H. Harada (Fujigaoka Hospital), Y. Morita (Kinki University), M. Matsuda (PL Hospital), H. Kashiwagi (Osaka University), T. Kiguchi (Chugoku Central Hospital), T. Masunari (Chugoku Central Hospital), K. Yamamoto (Yokohama City Minato Red Cross Hospital), T. Takahashi (Mitsui Memorial Hospital), and T. Takaku (Juntendo University) for providing patient samples. We thank K. Tanaka and Y. Shimamura for their technical assistance.

Finally I would like to extend my indebtedness to my family for their understanding, support and encouragement throughout my study.

References

1. Song WJ, Sullivan MG, Legare RD, Hutchings S, Tan X, Kufrin D, Ratajczak J, Resende IC, Haworth C, Hock R, Loh M, Felix C, Roy DC, Busque L, Kurnit D, Willman C, Gewirtz AM, Speck NA, Bushweller JH, Li FP, Gardiner K, Poncz M, Maris JM, Gilliland DG. Haploinsufficiency of CBFA2 causes familial thrombocytopenia with propensity to develop acute myelogenous leukaemia. Nat Genet 1999;23:166-75.

2. Owen CJ, Toze CL, Koochin A, Forrest DL, Smith CA, Stevens JM, Jackson SC, Poon MC, Sinclair GD, Leber B, Johnson PR, Macheta A, Yin JA, Barnett MJ, Lister TA, Fitzgibbon J. Five new pedigrees with inherited RUNX1 mutations causing familial platelet disorder with propensity to myeloid malignancy. Blood 2008;112:4639-45.

3. Ichikawa M, Asai T, Saito T, Seo S, Yamazaki I, Yamagata T, Mitani K, Chiba S, Ogawa S, Kurokawa M, Hirai H. AML-1 is required for megakaryocytic maturation and lymphocytic differentiation, but not for maintenance of hematopoietic stem cells in adult hematopoiesis. Nat Med 2004;10:299-304.

4. Blyth K, Cameron ER, Neil JC. The RUNX genes: gain or loss of function in cancer. Nat Rev Cancer 2005;5:376-87.

5. Matsuura S, Komeno Y, Stevenson KE, Biggs JR, Lam K, Tang T, Lo MC, Cong X, Yan M, Neuberg DS, Zhang DE. Expression of the runt homology domain of RUNX1 disrupts homeostasis of hematopoietic stem cells and induces progression to myelodysplastic syndrome. Blood

2012;120:4028-37.

6. Gaidzik VI, Bullinger L, Schlenk RF, Zimmermann AS, Rock J, Paschka P, Corbacioglu A, Krauter J, Schlegelberger B, Ganser A, Spath D, Kundgen A, Schmidt-Wolf IG, Gotze K, Nachbaur D, Pfreundschuh M, Horst HA, Dohner H, Dohner K. RUNX1 mutations in acute myeloid leukemia: results from a comprehensive genetic and clinical analysis from the AML study group. J Clin Oncol 2011;29:1364-72.

7. Harada H, Harada Y, Niimi H, Kyo T, Kimura A, Inaba T. High incidence of somatic mutations in the AML1/RUNX1 gene in myelodysplastic syndrome and low blast percentage myeloid leukemia with myelodysplasia. Blood 2004;103:2316-24.

8. Tang JL, Hou HA, Chen CY, Liu CY, Chou WC, Tseng MH, Huang CF, Lee FY, Liu MC, Yao M, Huang SY, Ko BS, Hsu SC, Wu SJ, Tsay W, Chen YC, Lin LI, Tien HF. AML1/RUNX1 mutations in 470 adult patients with de novo acute myeloid leukemia: prognostic implication and interaction with other gene alterations. Blood 2009;114:5352-61.

9. Ganly P, Walker LC, Morris CM. Familial mutations of the transcription factor RUNX1 (AML1, CBFA2) predispose to acute myeloid leukemia. Leuk Lymphoma 2004;45:1-10.

10. Liew E, Owen C. Familial myelodysplastic syndromes: a review of the literature. Haematologica 2011;96:1536-42.

11. Harada Y, Harada H. Molecular pathways mediating MDS/AML with focus on AML1/RUNX1 point mutations. J Cell Physiol 2009;220:16-20.

12. Harada Y, Inoue D, Ding Y, Imagawa J, Doki N, Matsui H, Yahata T, Matsushita H, Ando K, Sashida G, Iwama A, Kitamura T, Harada H. RUNX1/AML1 mutant collaborates with BMI1 overexpression in the development of human and murine myelodysplastic syndromes. Blood 2013;121:3434-46.

13. Yoshimi A, Goyama S, Watanabe-Okochi N, Yoshiki Y, Nannya Y, Nitta E, Arai S, Sato T, Shimabe M, Nakagawa M, Imai Y, Kitamura T, Kurokawa M. Evi1 represses PTEN expression and activates PI3K/AKT/mTOR via interactions with polycomb proteins. Blood 2011;117:3617-28.

14. Kirito K, Sakoe K, Shinoda D, Takiyama Y, Kaushansky K, Komatsu N. A novel RUNX1 mutation in familial platelet disorder with propensity to develop myeloid malignancies. Haematologica 2008;93:155-6.

15. Boutros R, Lobjois V, Ducommun B. CDC25 phosphatases in cancer cells: key players? Good targets? Nat Rev Cancer 2007;7:495-507.

16. Kastan MB, Bartek J. Cell-cycle checkpoints and cancer. Nature 2004;432:316-23.

17. Peng CY, Graves PR, Ogg S, Thoma RS, Byrnes MJ, 3rd, Wu Z, Stephenson MT, Piwnica-Worms H. C-TAK1 protein kinase phosphorylates human Cdc25C on serine 216 and promotes 14-3-3 protein binding. Cell Growth Differ 1998;9:197-208.

18. Lopez-Girona A, Furnari B, Mondesert O, Russell P. Nuclear localization of Cdc25 is regulated by DNA damage and a 14-3-3 protein. Nature 1999;397:172-5.

19. Satoh Y, Matsumura I, Tanaka H, Harada H, Harada Y, Matsui K, Shibata M, Mizuki M, Kanakura Y. C-terminal mutation of RUNX1 attenuates the DNA-damage repair response in hematopoietic stem cells. Leukemia 2012;26:303-11.

20. Krejci O, Wunderlich M, Geiger H, Chou FS, Schleimer D, Jansen M, Andreassen PR, Mulloy JC. p53 signaling in response to increased DNA damage sensitizes AML1-ETO cells to stress-induced death. Blood 2008;111:2190-9.

21. Preudhomme C, Renneville A, Bourdon V, Philippe N, Roche-Lestienne C, Boissel N, Dhedin N, Andre JM, Cornillet-Lefebvre P, Baruchel A, Mozziconacci MJ, Sobol H. High frequency of RUNX1 biallelic alteration in acute myeloid leukemia secondary to familial platelet disorder. Blood 2009;113:5583-7.

22. Balduini CL, Pecci A, Savoia A. Recent advances in the understanding and management of MYH9-related inherited thrombocytopenias. Br J Haematol 2011;154:161-74.

23. Fong PC, Boss DS, Yap TA, Tutt A, Wu P, Mergui-Roelvink M, Mortimer P, Swaisland H, Lau A, O'Connor MJ, Ashworth A, Carmichael J, Kaye SB, Schellens JH, de Bono JS. Inhibition of poly(ADP-ribose) polymerase in tumors from BRCA mutation carriers. N Engl J Med 2009;361:123-34.

24. Greif PA, Dufour A, Konstandin NP, Ksienzyk B, Zellmeier E, Tizazu B, Sturm J, Benthaus T, Herold T, Yaghmaie M, Dorge P, Hopfner KP, Hauser A, Graf A, Krebs S, Blum H, Kakadia PM, Schneider S, Hoster E, Schneider F, Stanulla M, Braess J, Sauerland MC, Berdel WE, Buchner T, Woermann BJ, Hiddemann W, Spiekermann K, Bohlander SK. GATA2 zinc finger 1 mutations

associated with biallelic CEBPA mutations define a unique genetic entity of acute myeloid leukemia. Blood 2012;120:395-403.

25. Ostergaard P, Simpson MA, Connell FC, Steward CG, Brice G, Woollard WJ, Dafou D, Kilo T, Smithson S, Lunt P, Murday VA, Hodgson S, Keenan R, Pilz DT, Martinez-Corral I, Makinen T, Mortimer PS, Jeffery S, Trembath RC, Mansour S. Mutations in GATA2 cause primary lymphedema associated with a predisposition to acute myeloid leukemia (Emberger syndrome). Nat Genet 2011;43:929-31.

26. Hahn CN, Chong CE, Carmichael CL, Wilkins EJ, Brautigan PJ, Li XC, Babic M, Lin M, Carmagnac A, Lee YK, Kok CH, Gagliardi L, Friend KL, Ekert PG, Butcher CM, Brown AL, Lewis ID, To LB, Timms AE, Storek J, Moore S, Altree M, Escher R, Bardy PG, Suthers GK, D'Andrea RJ, Horwitz MS, Scott HS. Heritable GATA2 mutations associated with familial myelodysplastic syndrome and acute myeloid leukemia. Nat Genet 2011;43:1012-7.

27. Hsu AP, Sampaio EP, Khan J, Calvo KR, Lemieux JE, Patel SY, Frucht DM, Vinh DC, Auth RD, Freeman AF, Olivier KN, Uzel G, Zerbe CS, Spalding C, Pittaluga S, Raffeld M, Kuhns DB, Ding L, Paulson ML, Marciano BE, Gea-Banacloche JC, Orange JS, Cuellar-Rodriguez J, Hickstein DD, Holland SM. Mutations in GATA2 are associated with the autosomal dominant and sporadic monocytopenia and mycobacterial infection (MonoMAC) syndrome. Blood 2011;118:2653-5.

28. Zhang SJ, Ma LY, Huang QH, Li G, Gu BW, Gao XD, Shi JY, Wang YY, Gao L, Cai X, Ren RB, Zhu J, Chen Z, Chen SJ. Gain-of-function mutation of GATA-2 in acute myeloid transformation of

chronic myeloid leukemia. Proc Natl Acad Sci U S A 2008;105:2076-81.